

**ISSUE 2/2014**

**Title Story // Model calibration as an optimization task**

An approach for optimizing turbomachinery designs

High frequency simulation

Sensitivity analysis of evacuation simulations

Model-based parameter identification

# RDO-JOURNAL

optiSLang

multiPlas

ETK

SoS

# FROM MODEL CALIBRATION TO RDO – STRATEGIC SETTINGS FOR VIRTUAL PROTOTYPING

In numerical simulations, abstract physical models are used to understand existing phenomena, to validate systems and to improve their designs. For the application of these models, for example, within a complex three-dimensional FE-simulation, the question often arises how the corresponding model parameters are to be chosen. Simple models allow parameters to be determined directly from experiments. In more complex models, such as for damage or material behavior, most phenomena can be only validated by analyzing a large number of parameters. Moreover, in many cases, it is not possible to decouple the influence of single parameters in order to identify them directly by appropriate tests.

For such tasks, in the field of engineering, inverse strategies are generated by using simulation models which correspond to the existing experimental geometry, constraints and test procedure. The unknown parameters are then determined by an iterative calibration between experimental data and simulation results.

During this calibration procedure, the identification of sensitive parameters plays a crucial part to avoid misleading values. Especially only parameters that have a significant impact on output variables can be identified and should therefore be selected for further steps of the calibration. Using optiSLang and methods of sensitivity analysis, these parameters can be determined efficiently. After the identification of a suitable set of input parameters and result variables, a successful model calibration can be conducted by using global and local optimization methods such as gradient-based or adaptive response surfaces as well as evolutionary and genetic procedures.

The analysis of the significance and sensitivity of the input parameters in the calibration process also reveals opportunities for system and product optimization. This approach is also suitable for the analysis and validation of non-linear system behavior. The methods can be used multidisciplinary and can be integrated in the virtual development process of all industrial fields.

In the title story of this issue, the application of optiSLang for parameter identification and model calibration as a special optimization task with signals will be introduced and illustrated by practical examples.

Apart from that, we again have selected case studies and customer stories about CAE-based Robust Design Optimization (RDO) applied in different industries.

I hope you will enjoy reading our magazine.

Yours sincerely



Johannes Will  
Managing Director DYNARDO GmbH

Weimar, November 2014

## CONTENT

**2 // TITLE STORY // MODEL CALIBRATION**  
Calibration of field data and simulation as an optimization task with signals

**12 // CASE STUDY // TURBO MACHINERY**  
An integrated approach for optimizing turbomachinery designs

**18 // CUSTOMER STORY // ELECTRICAL ENGINEERING**  
High frequency simulation

**22 // CASE STUDY // PROCESS ENGINEERING**  
Sensitivity analysis of evacuation simulations

**27 // CASE STUDY // MECHANICAL ENGINEERING**  
Model-based parameter identification:  
Cause and effect



## TITLE STORY // MODEL CALIBRATION

# CALIBRATION OF FIELD DATA AND SIMULATION AS AN OPTIMIZATION TASK WITH SIGNALS

Methods of sensitivity analysis and optimization with optiSLang can be used to improve a system design by understanding and validating its characteristic signal responses.

## Introduction

Signals are characteristic system responses that are critical in helping to understand, validate and improve the physical model of the system, as well as the system design itself by understanding the important parameters. Here, calibration means using field observations and simulation runs in order to estimate simulation model parameters or to update the uncertainty regarding these parameters. This can be formulated as an optimization task where the output parameters are signals and the target function is, for example, the sum of the square deviations of the signal from the testing and the signal from the simulation. The optimization task of identifying the right input parameters can then be formulated, for instance, to minimize the value of the target function by selecting the appropriate values for the input parameters. A simple example, however, shows that this can lead to a non-unique solution for the input parameters. Therefore, additional boundary conditions for the calibration can be very useful.

Knowing from the calibration the significance and sensitivity of input parameters, further optimization can be used to improve the system or product design. With the informa-

tion from the calibration, the design space can be adapted and appropriate surrogate models can be used that also respect nonlinear system behaviour.

In the case of strong scattering of test and/or simulation results, the identification task must be enhanced by stochastic analysis as the fit of single signals by design variables are no longer sufficient. Then, a parameter space has to be used where the input variables also have stochastic elements, like a stochastic distribution.

The technique of identifying the input parameters within an optimization task for the calibration of field data including measured signals and signals generated from the simulation can be used across all industries where virtual prototyping is important.

This article will give a first introduction and discusses some methods and measures used for sensitivity analysis and optimizations. The parameter identification as a special optimization task will be also shown by using two theoretical examples followed by three industrial applications. One of them will be explained in detail.

## Model Validation and Calibration with the Parameter Identification as an Optimization Task

Optimization using numerical simulations can, in general, be classified into two different categories: the first category is associated with the target to improve the functionalities of the product and the second category is to test and improve the model to more appropriately fit with the reality (Fig. 0).

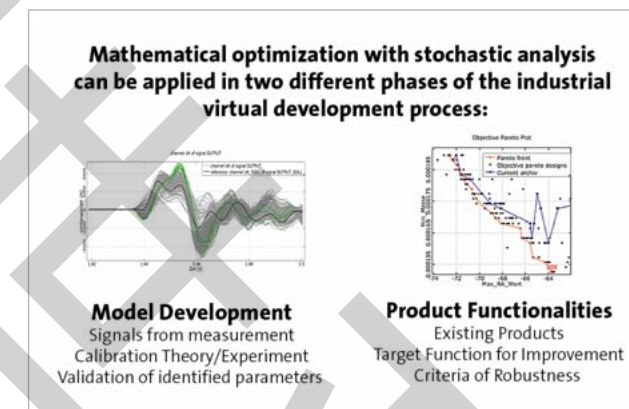


Fig. 0: Model calibration and improvement of product functionalities

While optimization has been already in wide spread usage for the improvement of product functionalities, the potential for the usage of similar optimization techniques to improve the quality of the model, typically with parameterization and calibration, is often not exploited.

The workflows that are used for the calibration of a model are similar to those used for the improvement of functionalities of the product. In both cases, it is recommended to start with a sensitivity analysis, especially when handling with a large number of parameters. A sensitivity analysis is used to study which input parameters have significant importance for which output parameters. These studies are also used to establish a meta model that approximates the output parameters as functions of the input parameters. This step can help to reduce the design space to the important parameters. For the criteria of importance of parameters and quality of the meta model, different statistical measures have been established. It is important that these meta models also include nonlinear dependencies of the parameters and that the prognosis quality is quantified. For the quantification of the quality of prognosis of such a model, the Coefficient of Prognosis, CoP, is introduced. With these CoPs, a nonlinear meta model can be selected that provides not only the best fit for the data but also the best model with respect to the ability for the best prognosis. Trying to only provide a model that best fits the data can lead easily to an overfitting and incapability of explaining further data. The model, based on the best CoPs, is the Metamodel of Optimal Prognosis, MOP. A typical workflow for the optimization of product functionalities is shown in Fig. 1. After the definition of the Design Space

X (the parameterization) and during the design of experiment (DOE), designs with different input parameters  $X_i$  are created. These different designs are solved, generating the values for the output parameter  $Y_i$ . These data samples can be used to establish the MOP, that can significantly reduce the design space to the important variables  $X_{red}$ , including nonlinear dependencies. Also, from the sensitivity analysis

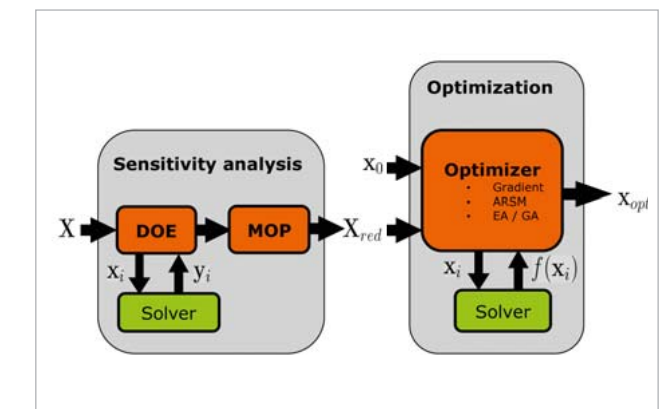


Fig. 1: A typical workflow for an optimization, starting with a sensitivity analysis for selecting the important parameters, followed by the optimization

a sufficient initial parameter set  $X_0$  is selected for optimization. Here, it is necessary to define at least one optimization function  $f(X_i)$ . Several optimization methods are available like gradient based, adaptive response surface, or evolutionary and genetic methods. Finally, an optimized set of input parameters  $X_{opt}$  is found.

The workflow for the calibration can be similar. A difference to the measurements, i.e. the sum of squared deviations of measured and calculated data for the corresponding time steps, is used as an optimization function. The identified parameter set is then the optimized set of input parameters  $X_{opt}$ .

## Two theoretical examples

There are not many optimization tools available that can handle different field measurements, i.e. time series for a pressure. Also, in general, they do not have the ability to include signals efficiently from the real test environment which is necessary for the target function of optimization. This is one of the main reasons that the potential of using optimization for parameter identification has not yet been fully exploited.

During the development of such a simulation model, the parameterization is the key to ensure its realistic behavior. The first example is a simple damped harmonic oscillator. This can be used to understand how signals can be handled. The example also illustrates that different optimization runs can lead to quite different parameter values. This is due to the fact that the solution can be realized with different values of the input parameters.

The basic input parameters for the calibration of the damped oscillator are the mass  $m$ , the initial kinetic energy  $E_{kin}$ , the damping  $c$  and the stiffness  $k$  (Fig. 2).

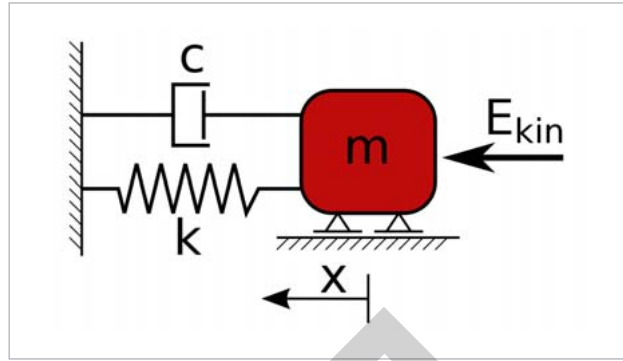


Fig. 2: Damped harmonic oscillator

The reference signal is taken from the displacement  $x$  over time for some parameters that are unknown in this example (Fig.3, red curve).

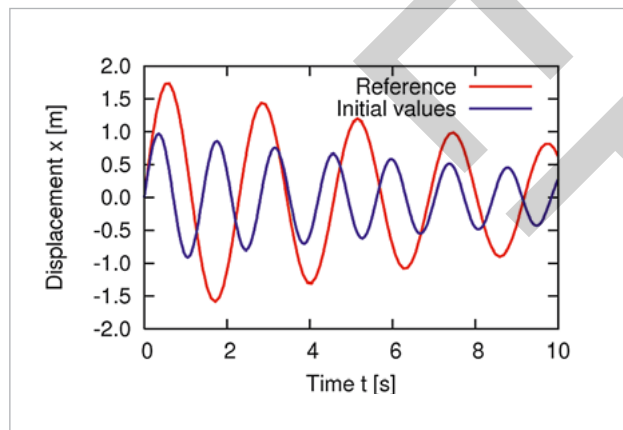


Fig. 3: The reference signal and the signal calculated from the initial values

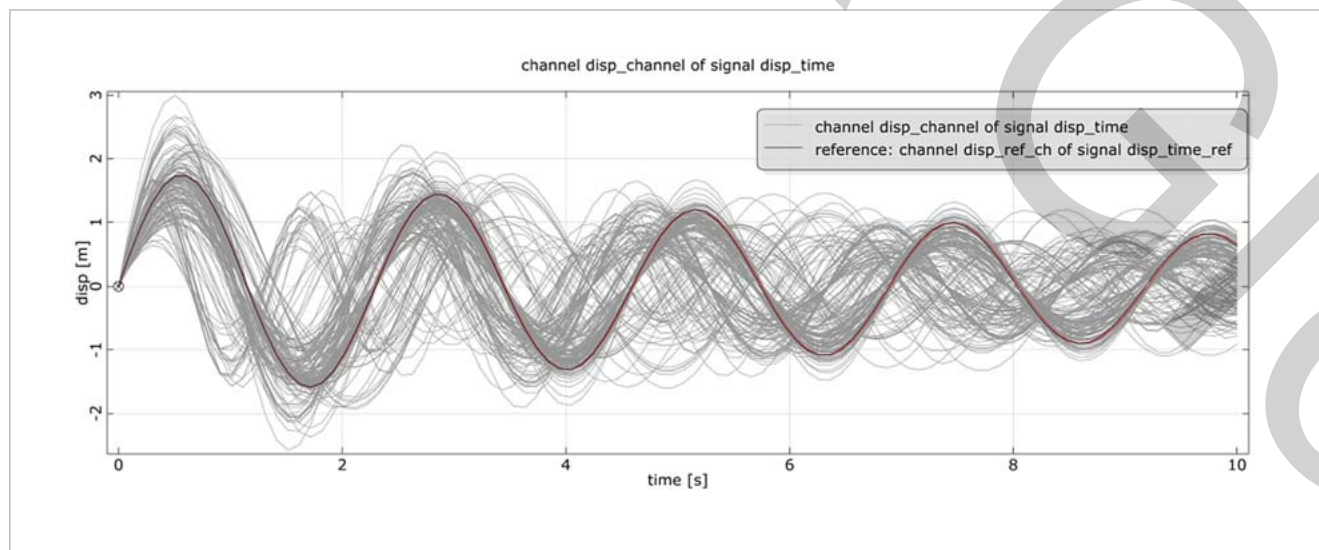


Fig. 4: The reference signal together with all signals from the sensitivity analysis

Equations for the damped oscillator:

$$\begin{aligned} m\ddot{x} + c\dot{x} + kx &= 0 \\ \ddot{x} + \frac{c}{m}\dot{x} + \frac{k}{m}x &= 0 \\ \ddot{x} + 2D\omega_0\dot{x} + \omega_0^2x &= 0 \end{aligned}$$

Analytic solution for the displacement:

$$x(t) = e^{-D\omega_0 t} \sqrt{\frac{2E_{kin}}{m}} \frac{1}{\omega} \sin(\omega t)$$

Undamped eigen-frequency  $\omega_0$ :

$$\omega_0 = \sqrt{\frac{k}{m}}$$

Lehr's damping ratio  $D$ :

$$2D\omega_0 = \frac{c}{m}$$

Damped eigen-frequency  $\omega$ :

$$\omega = \omega_0 \sqrt{1 - D^2}$$

The target for the optimization is to identify input parameters that generate a signal very close to the reference signal. Therefore, the objective function is the sum of squared differences between the displacement of the reference  $x^*$  and the displacement of the calculated solution  $x$  at  $n$  discrete time steps. Signals are generally discretized due to the measurement.

$$f(m, k, D, E_{kin}) = \sum_{i=1}^n (x_i^* - x_i)^2$$

The sensitivity study for this case shows that all input variables are significant. Thus, all signals from the designs of the design of experiment were processed during the sensitivity study. Illustrating the solutions for all these initial parameters, as shown in Fig. 4, often already provides an understanding of interesting frequency ranges for real world applications. Furthermore, some information are given about the feasibility of the parameter identification itself.

Running different optimizations lead to different sets of initial parameters as shown in Fig. 5.

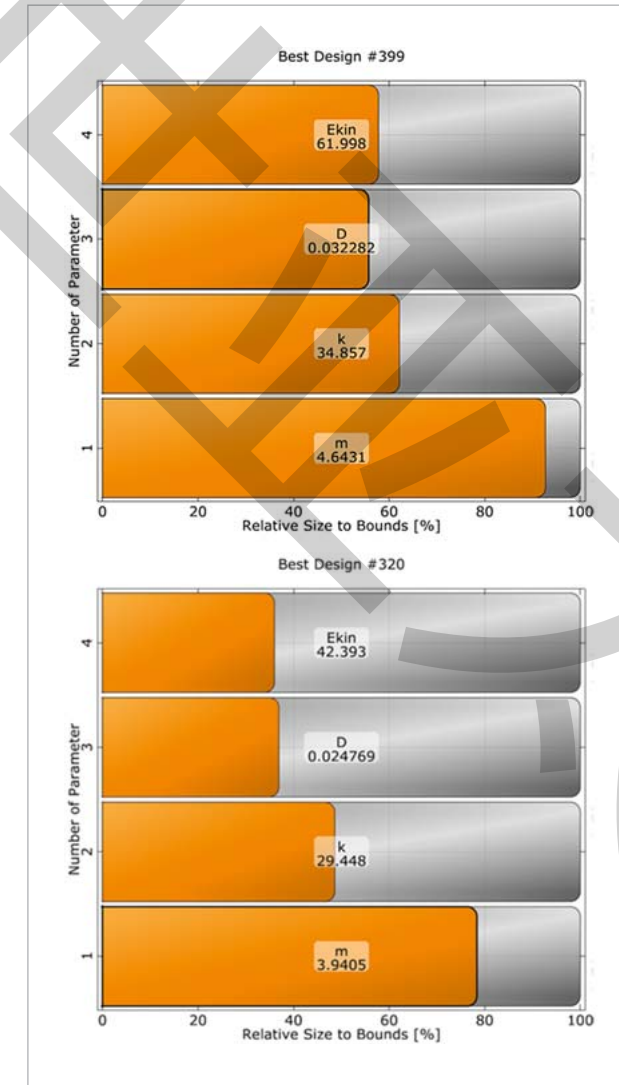


Fig. 5: Two different optimizations lead to rather different identified parameter values

Here, despite the different values for the parameters, both optimization runs lead to sufficient results showing only small differences compared to the reference signal (Fig. 6).

This non-unique solution for the identified parameters is due to the fact that the parameters  $E_{kin}$  and  $m$ , as well as  $m$  and  $k$  appear only pairwise in the solution for the displacement. It is only their ratio that matters for the solution.

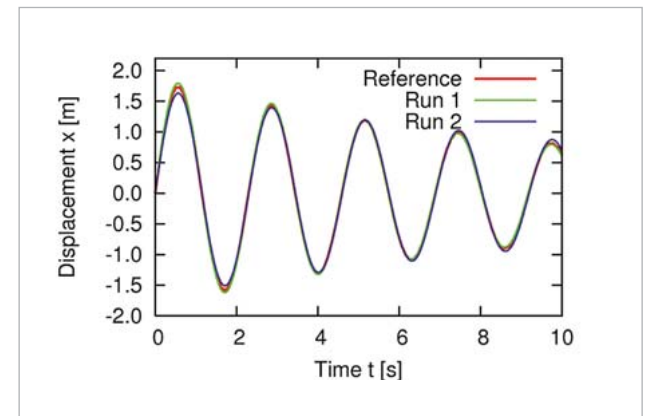


Fig. 6: The identified parameter values from both optimizations lead to a sufficient approximation of the reference signal

Therefore, a unique solution can be generated by having, for example, a constant mass value for the optimization. This example is shown in more detail also for training purposes with signals in an optiSlang tutorial available from Dynardo and currently included in the software delivery. The second example is a simplified CFD test model where a reference vector of the 12 outflow velocities exists. The optimization task is to find the set of 10 input parameters for the pressures (Press\_1 ... Press\_10) that come close to the outflow velocities (Fig.7).

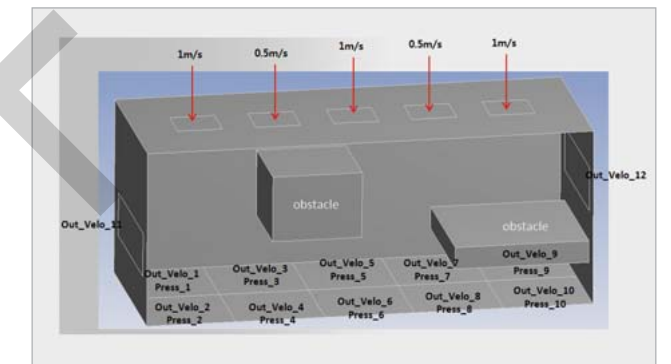


Fig. 7: A CFD example of a box with two obstacles

The optimization function to minimize, similar to the signal function for the damped harmonic oscillator case, is the squared deviation of the reference velocities  $Ref\_Velo_i$  and the velocities  $Out\_Velo_i$  from the calculated solution:

$$\sum_{i=1}^{12} (Ref\_Velo_i - Out\_Velo_i)^2$$

Also, in this case it is important to have additional constraints. It was chosen that each output parameter is close enough within 10% of the corresponding reference output parameter:

$$abs((Ref\_Velo_i / Out\_Velo_i) * 100 - 100) < 10$$



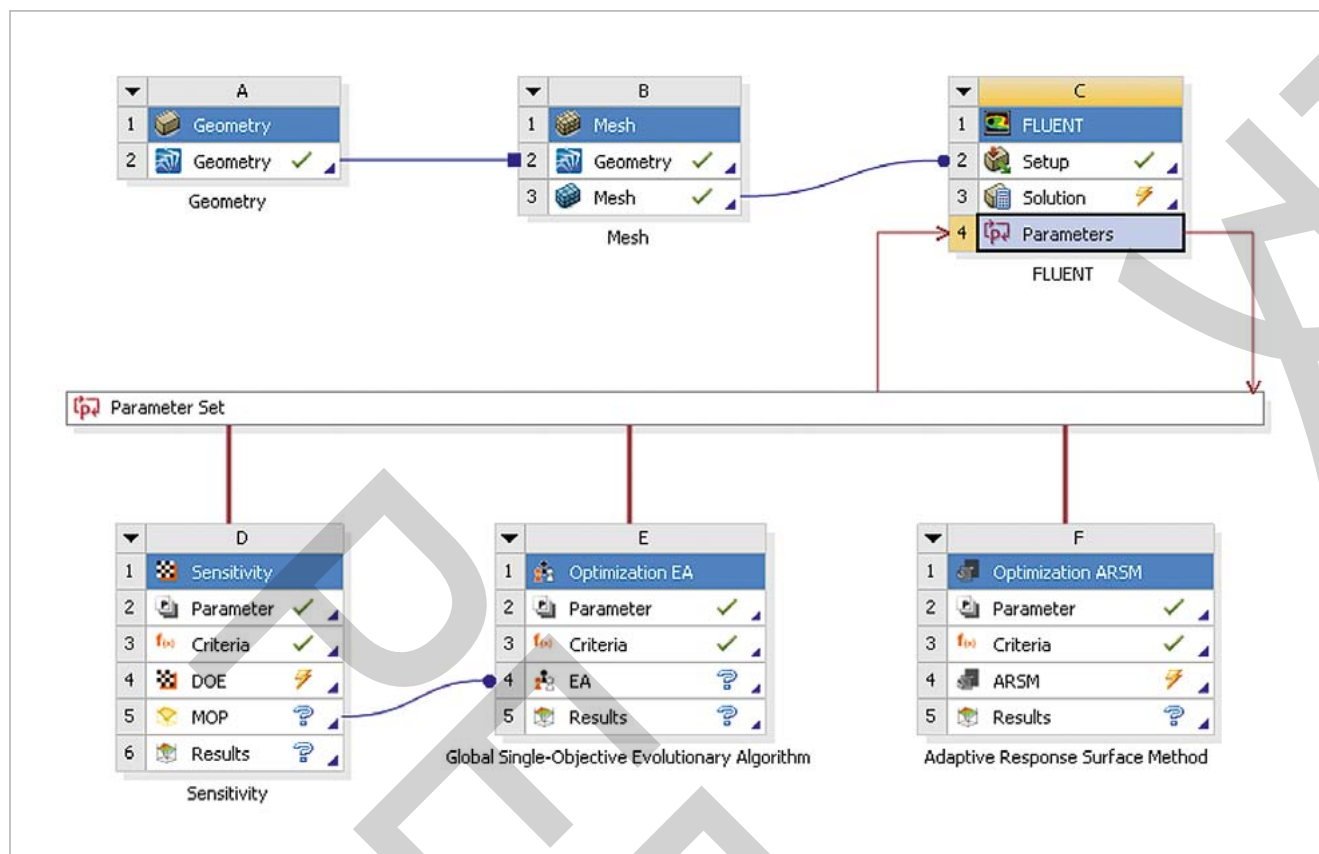


Fig. 8: The ANSYS Workbench set up with optiSlang inside ANSYS Workbench for the CFD example of a box with two obstacles

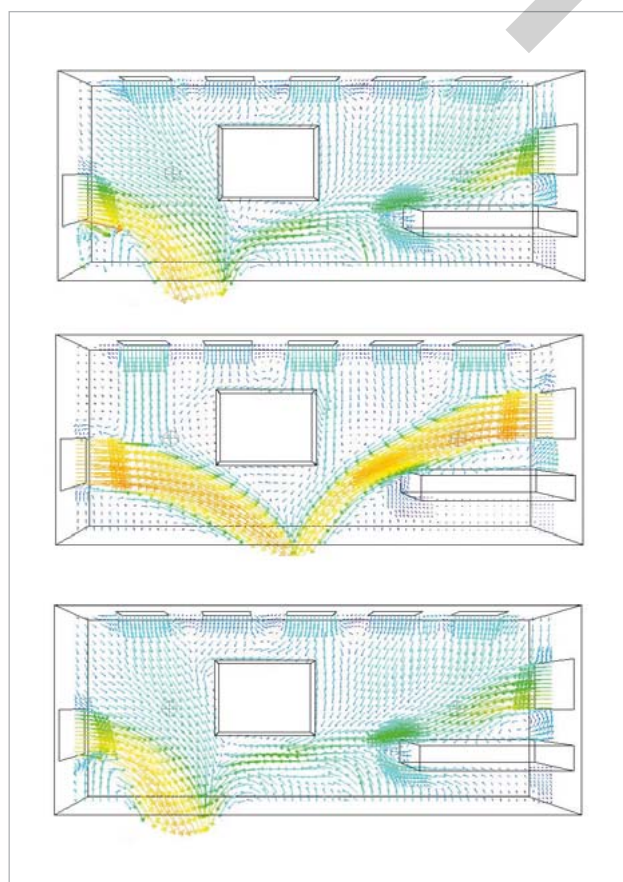


Fig. 9: Reference solution (top), initial solution (middle) and optimized solution (bottom) showing the velocity vectors colored by velocity magnitude

This problem was solved with optiSlang inside of ANSYS Workbench. The complete workflow is shown in Fig. 8. The solution was found with an Adaptive Response Surface Method. In general, this method is recommended for a small number of continuous input parameters (Fig. 9).

### Practical Applications

The field of practical applications for model calibration by parameter identification cover a broad range. Some publications are available from the online library of Dynardo, showing applications from different industrial areas like civil engineering (Zabel and Brehm, 2008), automotive (Will, 2006) and oil & gas (Will, 2010). In this article, the focus will only be on two applications with signals, some progresses we have made for an NVH automotive application and a new model calibration for a nuclear waste depository analysis.

### Calibration and Optimization of Driving Comfort Behaviour

In product development of luxury cars, Noise Vibration Harshness (NVH) plays a very important role. Driver, co-pilot and passenger on the back seats should feel very comfortable during any driving conditions. Therefore, the calibration of virtual models to available test data and the reduction of noise levels inside the car cabin is an important task of the virtual prototyping. For the formulation of a successful calibration design space as well as a successful objective function, two challenges need to be met. First, a very large

number of variables may have an influence on the passenger car air vibration. Second, the frequency signals show a very large number of vibration modes. As a result, the selection of the main influencing parameters and the signal processing to extract response values which belong to one vibration mode are a very important part of the calibration process. In the example, we start with a variation space of 485 sheet metal thicknesses of all body parts which might have an influence. Fig. 10 shows the variation of one of the sound pressure signals of 200 Latin Hypercube samples of the sensitivity analysis (Fig. 10).

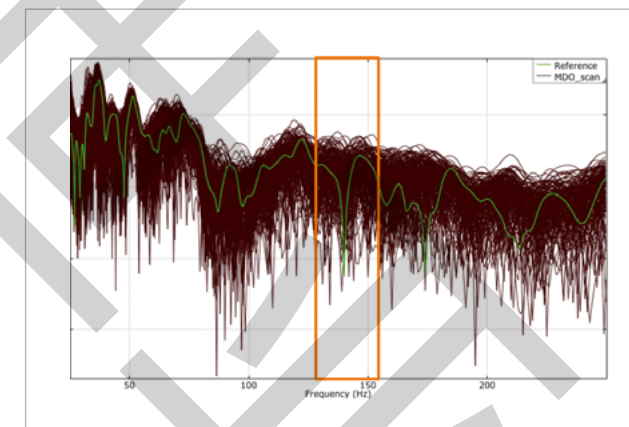


Fig. 10: Variation of sound level, green – reference, black – 200 samples of the sensitivity analysis

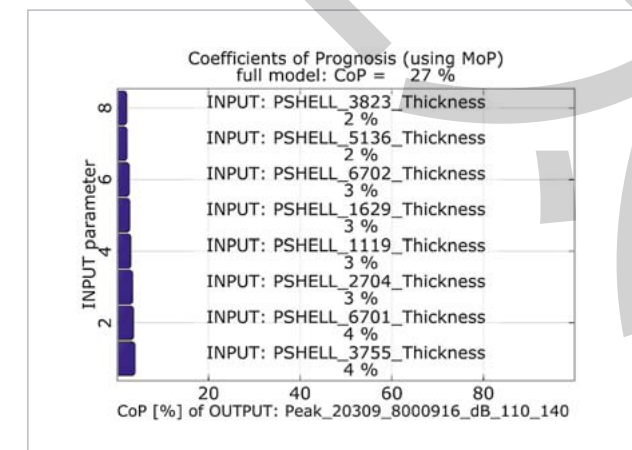


Fig. 11: CoP value of the peak sound level in the frequency window 110 to 140 Hz, sensitivity study using 485 variables

Having the signal variation window, the frequency window was defined to extract the peak sound values which correspond to the vibration mode of interest. Note that because of stiffness variation, the frequency and the sound value are varying at the same time and we need to adjust the extraction windows to avoid mode switch of important vibration modes within one extraction window.

Unfortunately, the CoPs for the variation of the peak sound level are below 30%, which indicate that only the impor-

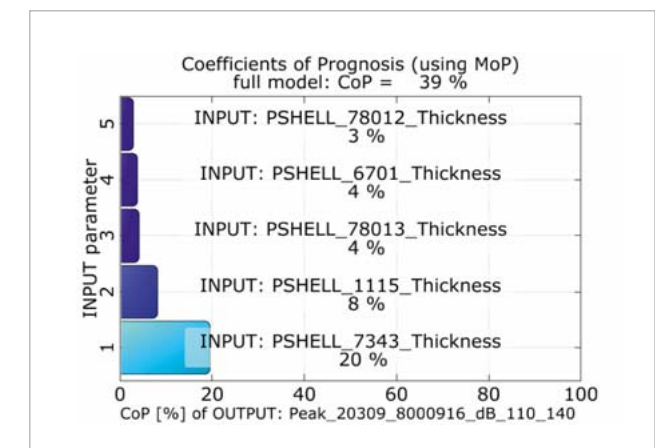


Fig. 12: CoP values of the peak sound level in the frequency window 110 to 140 Hz, sensitivity study using 37 variables

tant variables for less than 30% of the total variation were identified. It is our experience for this kind of identification task, that increasing of sampling to 300 or 400 designs or alternative extraction windows does not increase the CoP levels significantly. The main reason for the small CoP levels is that the pressure sound levels are influenced by mechanisms of 10 to 20 variables. To identify these mechanisms out of 500 variables, a very large number of sample points will be necessary (Fig. 11).

Therefore, the CoP values from the first sensitivity analysis were used to reduce the design space manually. Those 37 variables were selected which showed significant CoPs for any of the response values of interest and repeated the sensitivity study in the reduced design space. At the second sensitivity study using 37 variables, the variation interval of the peak value within the frequency window 110 to 140 Hz is 80% compared to the first sensitivity study using 485 variables. That approved the CoP based selection of important parameters. In the reduced space, higher CoP values of the full model are close to 40% and higher CoP values of single variables are identified (Fig.12).

Within the reduced design space of 37 important variables, the main contributors could also be identified for the other important frequencies and positions. Furthermore, the calibration to the reference signal was performed successfully. Of course, after having a model which shows sufficient forecast quality to measurements, the next step in the virtual prototyping will be the optimization. Here, the minimization of peak sound pressure levels is shown in Fig. 13 (see next page).

### Calibration of a Nuclear Waste Depository Model

During the research for the safeness of nuclear waste depositories, heating experiments are performed in underground laboratories in order to understand the thermal-hydraulic-mechanical (T-H-M) interactions. In these experiments, the change due to the heat energy input over time of temperature, pore water pressure and stress fields are measured.



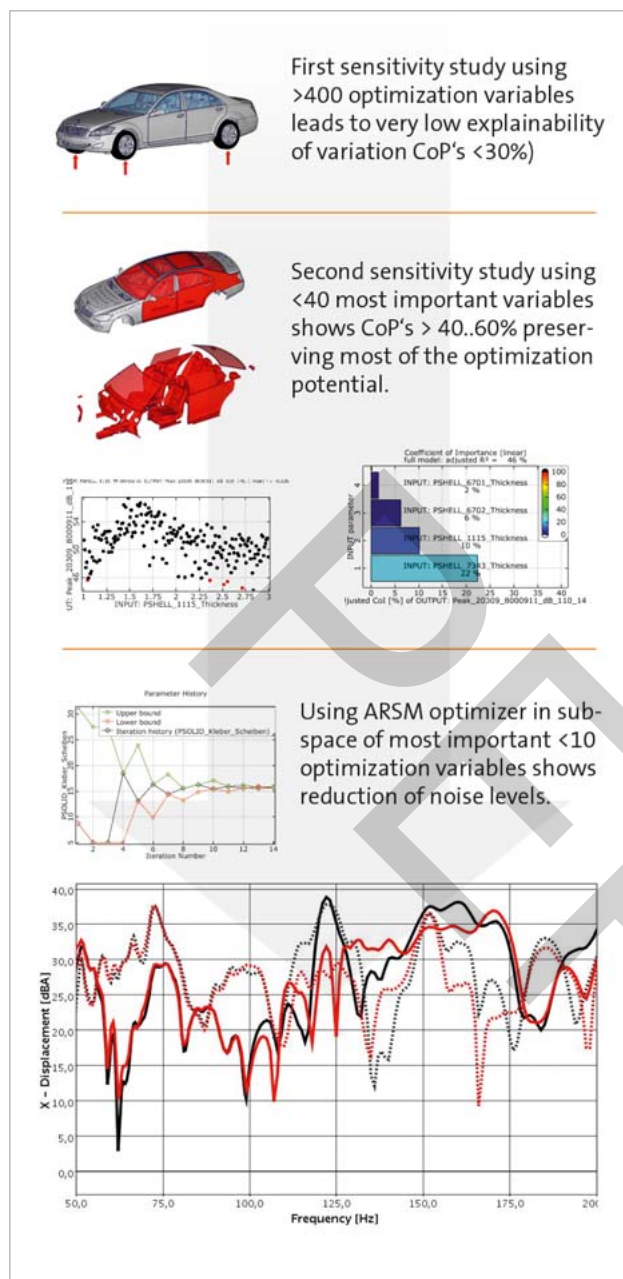


Fig. 13: Overview of the process for an optimization using the same sensitivity study but selecting only the eight most important variables for the optimization (by courtesy of DAIMLER AG)

The DBE TECHNOLOGIE GmbH develops, in cooperation with the Dynardo GmbH, simulation models that are able to comprehend these interactions in claystone. An important component of these developments is the calibration of the models with respect to the results of the measurements. The heating experiment has been simulated with a T-H-M coupled 3-dimensional finite element analysis with ANSYS and multiPlas. Therefore, special routines from the poro-elasticity theory, thermal-hydraulic coupling and thermal-mechanical coupling in isotropic and anisotropic claystone formations were developed and implemented in ANSYS. For the sensitivity analysis and for the parameter identification, optiSLang was used. Due to the complexity of the T-H-M phenomena, about 30 model parameters were

used. In this case, it was essential for the successful calibration of measurement and simulation to use the powerful algorithms and filter strategies for large parameter spaces of optiSLang and the achieved short calculation times due to efficient numerical algorithms of ANSYS with multiPlas. In the sensitivity analysis, the material parameters (including parameters for the coupling) have been varied within physical possible boundaries.

From the experiment temperature and pore water pressure data are available for 17 measurement points during the heating, as well as before the heating. Due to uncertainties in the process before the heating, the calibration and parameter identification was restricted to the heating process itself. For the evaluation of the sensitivities, the relative pore water pressures discrete time values were used. By the selection of these output values, statements became possible for the sensitivity at the beginning and at the end of the heating, as well as for the time when the pore pressure reached the maximum.

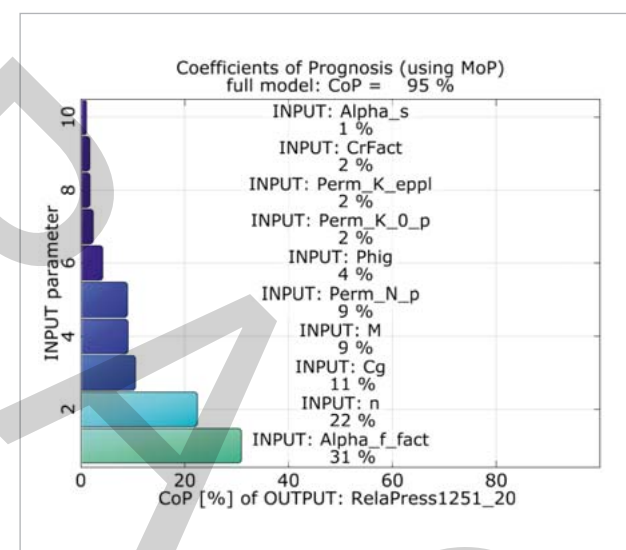


Fig. 14: High CoPs are an indicator for the sufficient quality of the model

The total Coefficients of Prognosis (CoP) show high values of above 85% (Fig. 14). This underlines that the physical phenomena are very well explainable through the identi-

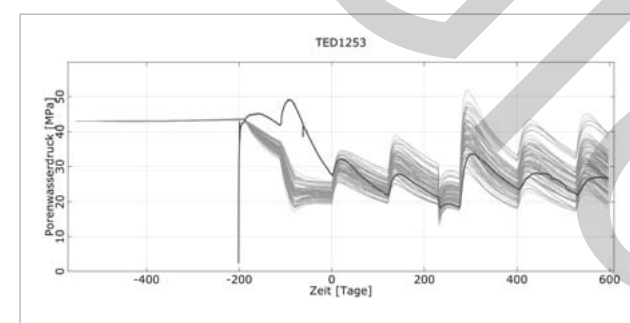


Fig. 15: Pore water pressure at measurement point TED1253, as a signal over time, compared with the simulated signals of the sensitivity analysis

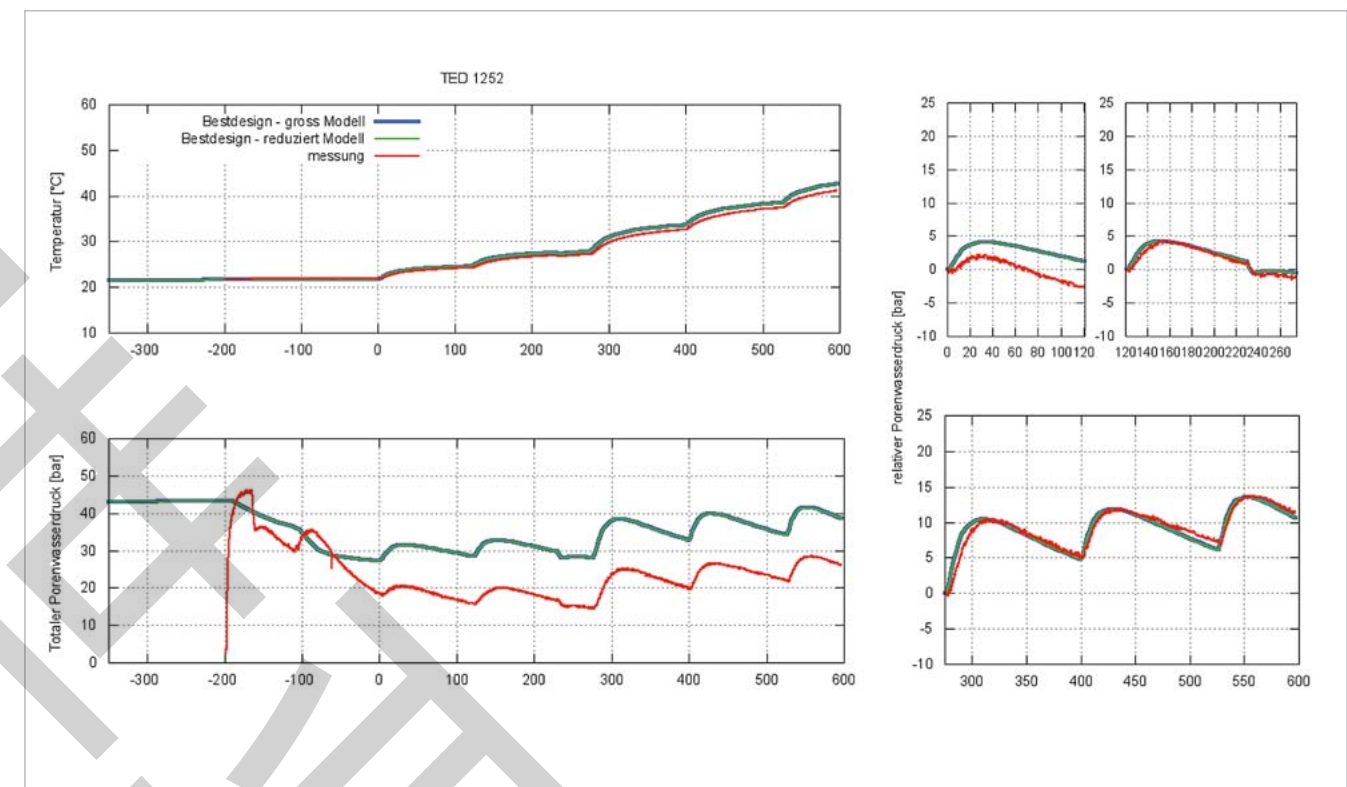


Fig. 16: Comparison of measurement vs. simulation at measurement point TED1252 after parameter identification. Top left: temperature over time, bottom left: total pore water pressure, right: relative water pressure for the three phases of heating.

fied correlations and also indicates that the correct important parameters for establishing the model were used.

By comparison of the scatter range of the calculated signals with the signals from the measurement (Fig. 15), statements about the quality of the model and the possible calibration of the model with the measurement are possible. If the scatter range of the calculated values is surrounding the measured values, then a successful calibration within the selected boundaries of the parameters can be possible. The figure shows that this is possible from the start of the heating experiment ( $t=0$ ).

For the parameter identification, the optimization selected a set of input parameters leading to a good approximation of the measured signals of the temperature and the pore water pressure over time. Parameters that only showed a negligible sensitivity have not been varied through the optimization for the parameter identification. They have been set to their reference values.

The comparison of the measured and calculated time signals of temperature and pore water pressure (s. figure 16) shows that with the identified parameter for the model the physical phenomena could be simulated very plausibly and a very good calibration with temperature and pore water pressure was reached.

## Outlook

This article explained, using theoretical and practical cases, how the calibration of a model with parameter identification can be treated as an optimization problem including signals. These techniques will become most probably an important standard technology for the development of more accurate models for the simulation.

In the following article we present a more detailed example for model calibration and parameter identification where also the varying influences of the parameters for the different stages of an experiment are analyzed. Additionally, in this example, the parallel coordinate plot of optiSLang is used to understand which parameters are really good identifiable.

Author // Roland Niemeier (Dynardo GmbH)

Source // [www.dynardo.de/en/library](http://www.dynardo.de/en/library)

presented at the NAFEMS World Congress 2013,  
[www.nafems.org](http://www.nafems.org)



## Example: Identification of concrete fracture parameters from a wedge splitting test

The following example will explain the basic procedure using a wedge splitting test regarding Trunk [Trunk1999]. During this experiment, a pre-slotted specimen was loaded vertically along a predefined crack edge. With this setup, the experimental measurement of the post-cracking behavior was possible.

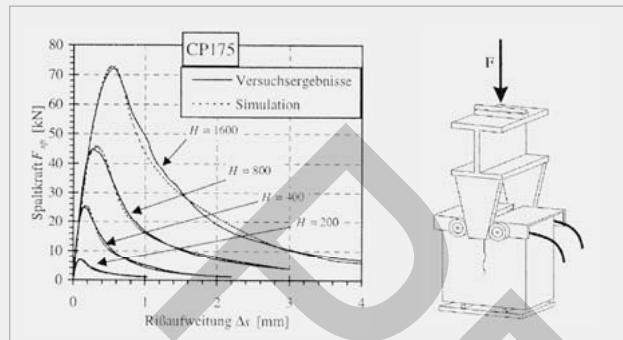


Fig. 1: Wedge splitting test regarding Trunk, experimental setup and measured load-displacement curves for different specimen

The simulation model represents the specimen as a linear elastic continuum containing 2D plane-stress elements. The theoretical crack evolution was represented by 2D interface elements, whereby the softening behavior was modeled using a common bilinear softening law. The tensile strength  $f_t$  and the specific fracture energy  $G_f$  as well as the two shape parameters  $\alpha_{ft}$  and  $\alpha_{wc}$  describing the kink of the bilinear curve, serve as fracture parameters. The simulation was conducted path-controlled causing a steadily increased crack opening width. In the first step, a sensitivity analysis was performed. Here, the Young's modulus  $E$ , the Poisson's ratio  $\nu$  and the four fracture parameters were varied. As a design-of-experiment-scheme, a correlation-optimized Latin Hypercube Sampling was used. The simulation curves were

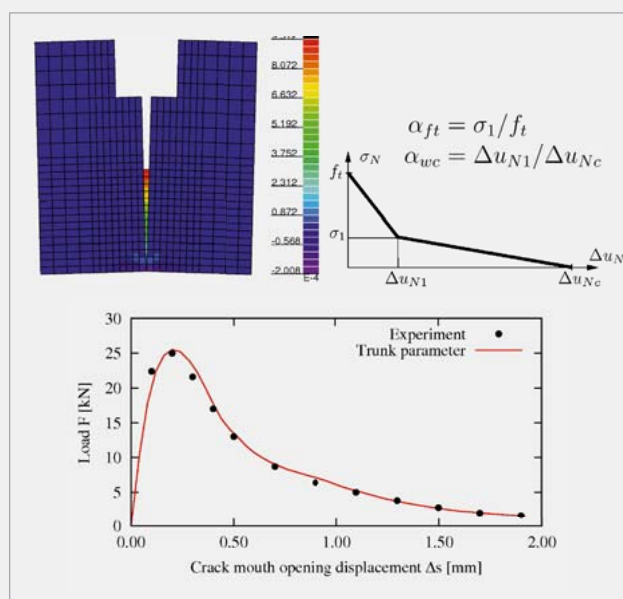


Fig. 2: 2D simulation model (top left) with stress history vertical to the crack surface, bilinear softening model (top right) and simulative load-crack opening curve (bottom)

calculated and imported in optiSlang via a signal module for each of the 100 samples. The curves showed a good adoption of the estimated range of values according to the reference signals (Fig. 3). An identification with the estimated parameter ranges was possible. Furthermore, the influence of the model parameters on the response variables was analyzed using the Metamodel of Optimal Prognosis.

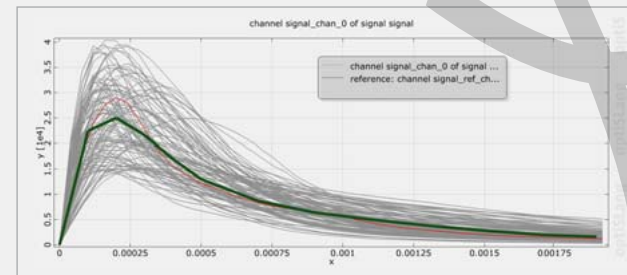


Fig. 3: The range of 100 simulation curves from the Latin Hypercube Sampling covers the reference signal from the measurements sufficiently.

Fig. 4 shows the meta-model and Fig. 5 the parameter influence concerning the sum squared errors. It can be seen that the Poisson's ratio and one of the form parameters most likely cause no effect. However, the approximation quality was not satisfying and less important factors were not identified due to insufficient sampling points. To ensure that only parameters without influence were excluded from the

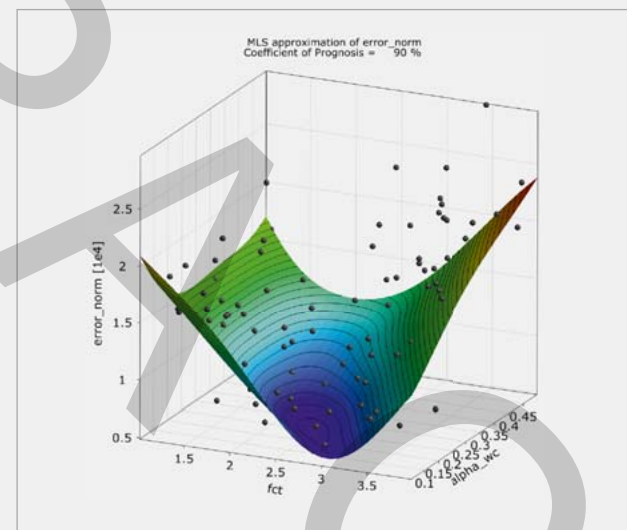


Fig. 4: Approximation of the sum of squared errors using Moving Least Squares

identification, effects appearing during the softening process were analyzed more detailed. The loads at the reference points (Fig. 2) were extracted from the signals of the simulation model and, for each value, a sensitivity analysis was conducted. This could be done without any further simulation runs because the additional scalar values were just extracted from the calculated response signals. The displacement dependent sensitivity indices are shown in Fig. 6. It illustrates that the Poisson's ratio had no influence. Apart from that, all parameters caused at least a partial effect during the simulation. The conclusion can be drawn that all parameters except the Poisson's ratio were identifiable from the measurement data.

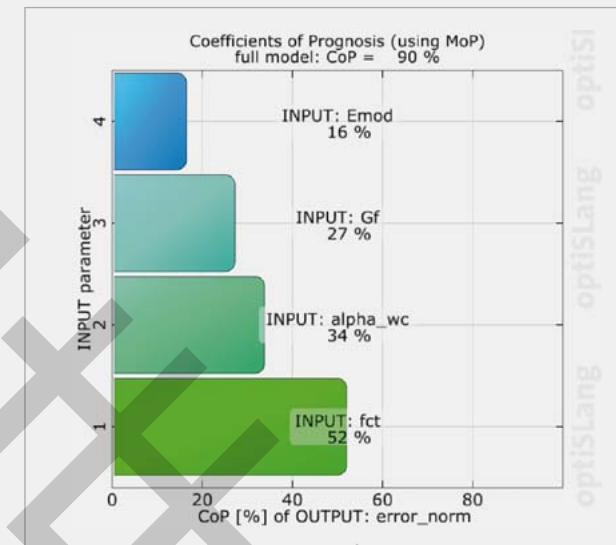


Fig. 5: Variance-based sensitivity indices of the parameters to be identified (right)

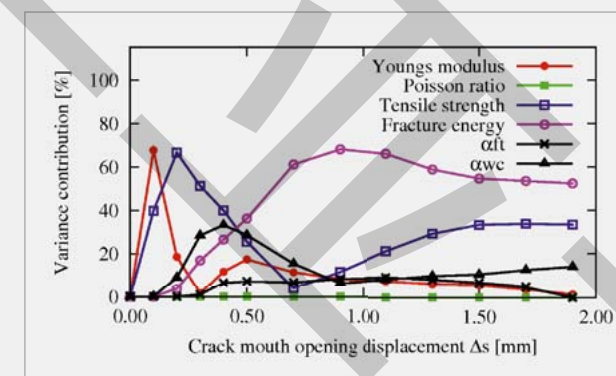


Fig. 6: Sensitivity indices for all input parameters depending on the crack opening width

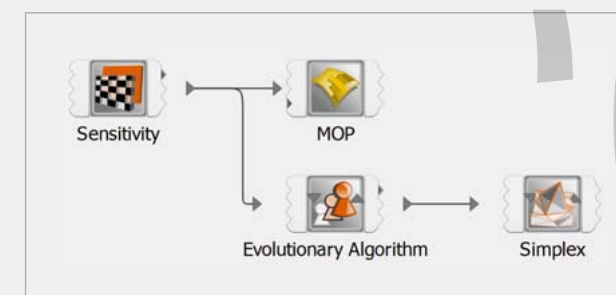


Fig. 7: Flow chart of identification: the sensitivity analysis generated the DoE designs as well as a response surface model using the Metamodel of Optimal Prognosis. For global search, the best designs served as a start population for the Evolutionary Algorithm. The resulting best design was then used as the starting point of the local search using simplex Nelder-Mead.

The next step was the conduction of a global optimization using an Evolutionary Algorithm with the 10 best designs of the sensitivity study as a start population. This improved the convergence of the optimization process significantly. The best design was then used as a start design for a local optimization. For the local search, the Simplex-Nelder-Mead method was used (Fig. 7). Finally, the issue of ambiguity was verified in detail. For this purpose, the designs of the local optimization were depicted as a parallel coordinates plot. The range of the sum of squared errors was restricted. Thus, only

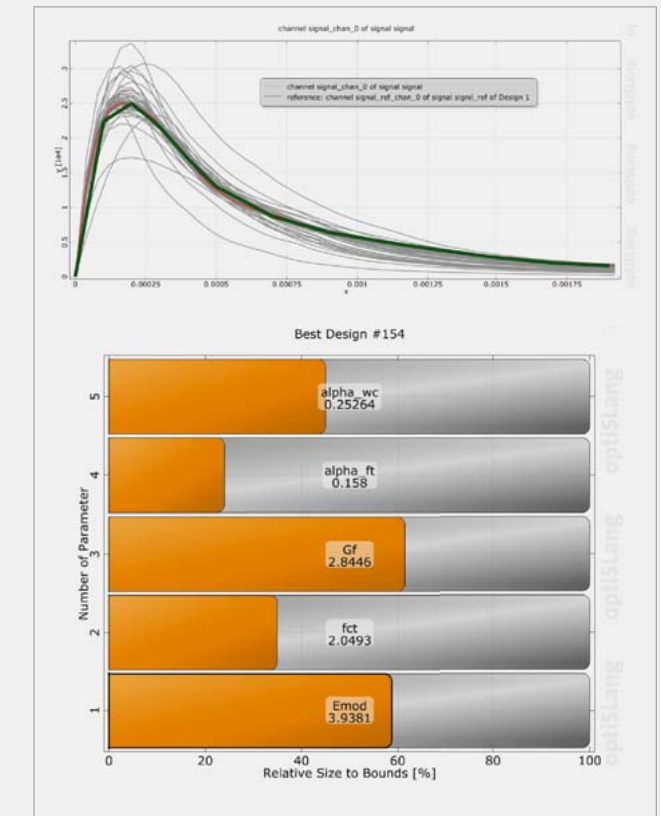


Fig. 8: Optimized simulation curves and optimal parameters showing a very good correlation between measurement and simulation

simulation curves with a very similar course were shown. In reference to the accompanying parameter ranges, it was illustrated that the modulus of elasticity, the tensile strength as well as the fracture energy show very small intervals and were sufficiently identi-

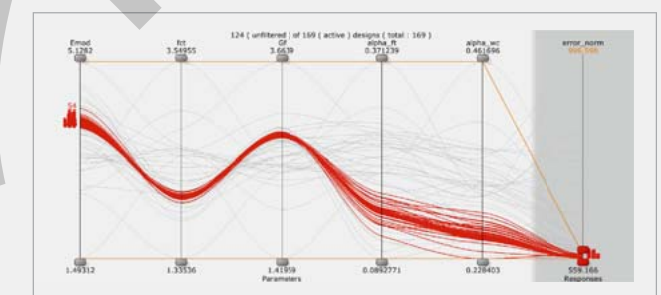


Fig. 9: Parallel coordinate plot of the best optimization designs for all considered material parameters and the sum of the least squares.

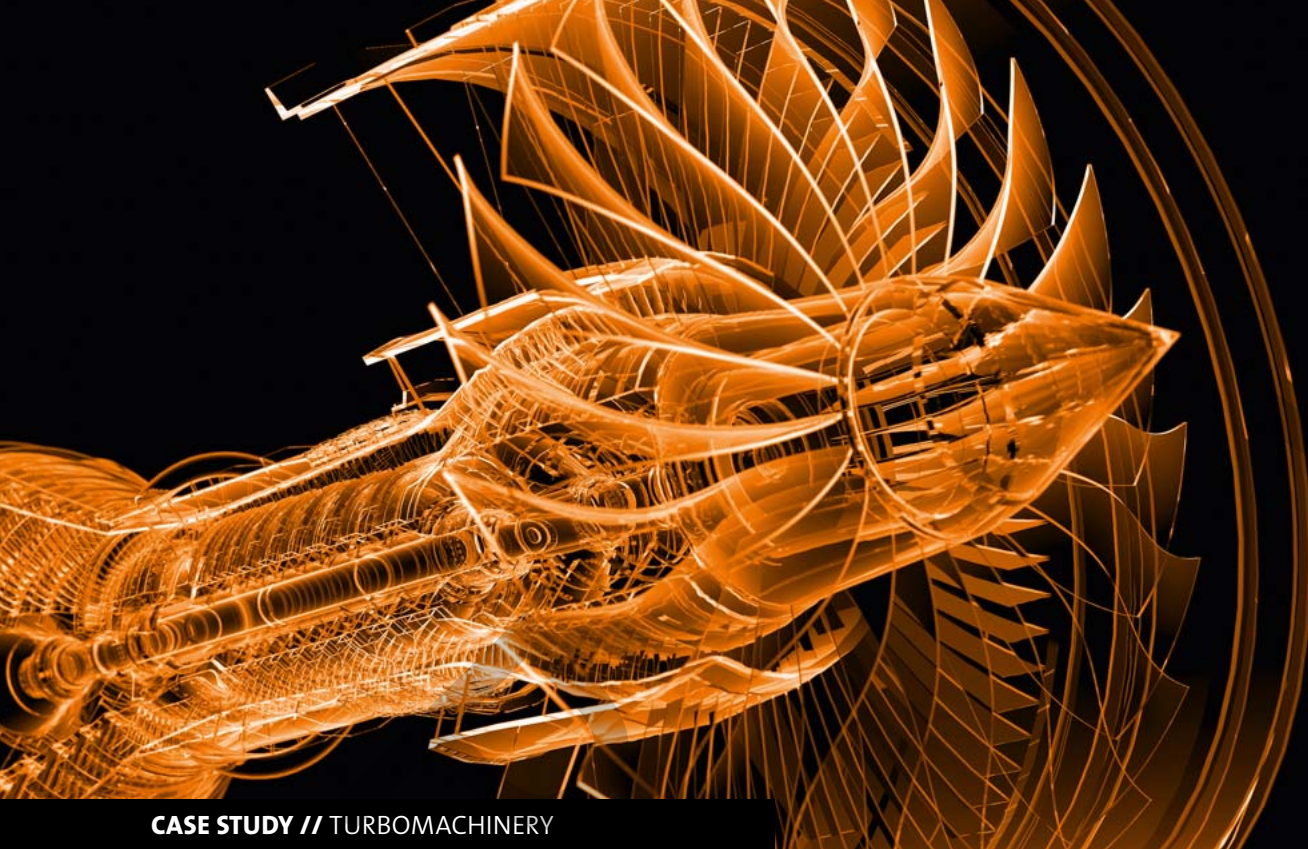
fiable. The two shape parameters showed very similar result diagrams applied with a larger deviation margin. Therefore, they were not sufficiently identifiable from using the available measurement points. Here, the consideration of further experimental data would certainly improve the validity.

**Author //** Thomas Most (Dynardo GmbH)

**Source //** [www.dynardo.de/en/library](http://www.dynardo.de/en/library)

[Trunk 1999] Trunk, B., "Einfluss der Bauteilgröße auf die Bruchenergie von Beton", Dissertation, Eidgenössische Technische Hochschule, Zürich, 1999





## CASE STUDY // TURBOMACHINERY

## AN INTEGRATED APPROACH FOR OPTIMIZING TURBOMACHINERY DESIGNS

ANSYS and optiSLang provide a new approach to turbomachinery design by applying numerical simulation and optimization based on objective and reproducible methods.

### Introduction

Turbomachinery design today primarily relies on the intuition of experienced designers to determine which angle needs to be modified to improve the design. A new integrated approach to turbomachinery design based on objective and reproducible methods will be introduced in this article. It is intended for engineers and require neither mathematical expertise nor many years of experience to be applied. This optimization method is capable of scanning the entire design space in order to survey it completely and to identify local optimums. By this initial step, an algorithm generates more detailed simulations which represent the optimal solution with a high level of accuracy.

### Challenges in turbomachinery design

There are many variables involved in turbomachinery design, each causing a complex effect on the final product performance. Today's most common design methods start with a one-dimensional analysis and include engineering experience to obtain an initial design having a reasonable efficiency level of approximately eighty five percent. The next step is usually a computational fluid dynamics (CFD)

simulation. This provides a more detailed look at the flow velocity as well as direction and pressure conditions. It also identifies issues such as recirculation which cannot be detected with one-dimensional analysis. However, to run such a simulation takes normally a considerable amount of time and each run provides diagnostic information about just one design iteration.

Experienced turbomachinery designers can review CFD simulation results and make educated guesses about which design modification might be possible to generate a significant improvement of product performance. Such designers are capable of increasing efficiency up to almost ninety percent. However, there are just a few engineers having the experience needed to intuitively understand which parameters need to be changed to improve the design.

Even these experts are rarely capable of achieving a 90%+ efficiency level which can be found in today's best-in-class designs. Attaining this level requires a much more sophisticated analytical process. By using CFD, hundreds or even thousands of potential designs can be analyzed automati-

cally. Even with the latest computing hardware, it is still a challenge to deal with the large amount of computing time and resources required to conduct such simulations. Consequently, turbomachinery designers want to address this challenge with optimization algorithms that reduce the number of simulation runs required to explore the design space and to identify the best designs. There are many different optimization algorithms delivered as black box applications which often require considerable mathematical expertise to operate. These algorithms can also fail to find an optimal solution because of limitations in their capacities.

Due to the complexity of turbomachinery development, parameters leading to optimal solutions are often located in spaces surrounded by relatively inefficient designs. Therefore, optimization algorithms that push efficiency towards higher levels often fail to identify the optimal solution, because, while avoiding surrounding low-efficiency designs, they tend to shift temporarily towards design spaces of reduced efficiency.

Another fact making turbomachinery development complicated is that the structural design process must be performed simultaneously in order to ensure the design will be able to handle the resulting loads. Typically, design and structural engineers work in different departments with different tools. Both frequently make design modifications. This might create the risk that the two groups work on different files causing extra expenses and delays in the downstream process.

### Integrated approach

This article will demonstrate an integrated approach for optimizing the design of a centrifugal compressor while ensuring sufficient robustness towards manufacturing variations. The design geometry, including the blades and hub body, was defined in ANSYS BladeModeler, which is fully integrated into the ANSYS Workbench environment. The design was defined in a number of 2-D sketches, either at span-wise positions or at arbitrary user-defined positions. Thus, a full 3-D design was interactively generated providing quantitative information such as blade angles and throat area.

In this application, the geometry of the blades was defined by the meridian flow path consisting of two parametric sketches, one for the hub and another for the shroud. The location of the leading and trailing edges for the rotor, as well as the return guide vane, were defined based on the meridian plane. Angle and thickness distribution of the hub and shroud layer defined the shape of the blades. There were a total of 17 input parameters, as shown in Fig. 1b.

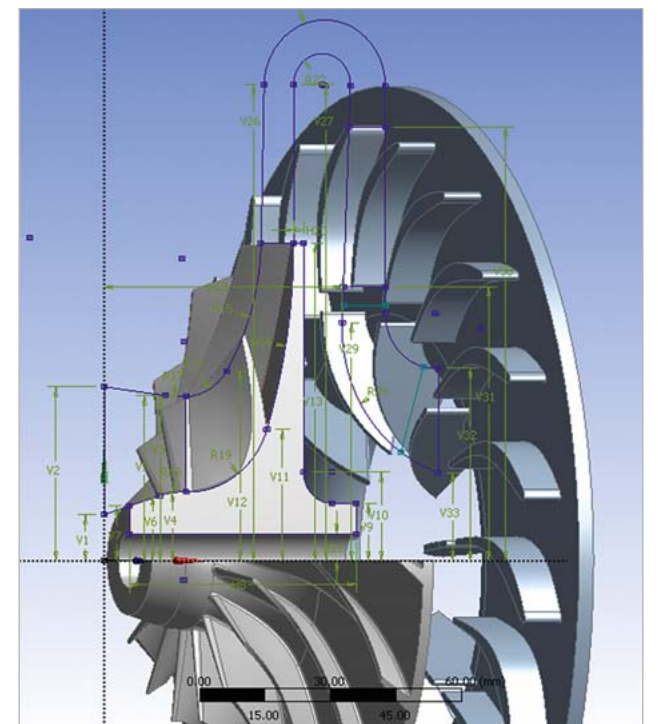


Fig. 1a: Parametric geometry

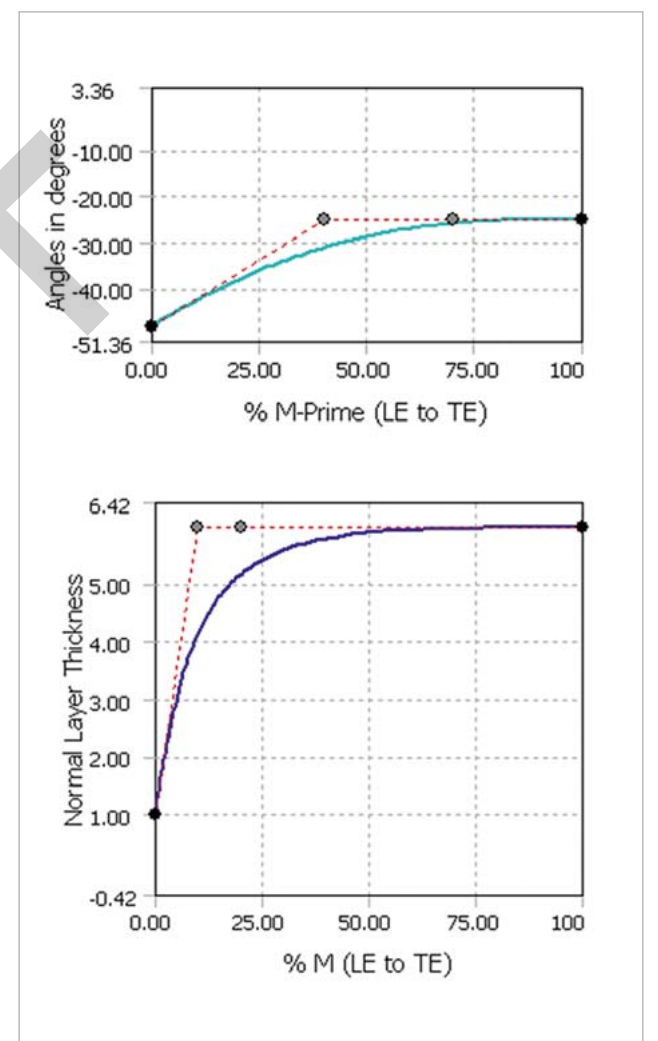


Fig. 1b: Input parameters



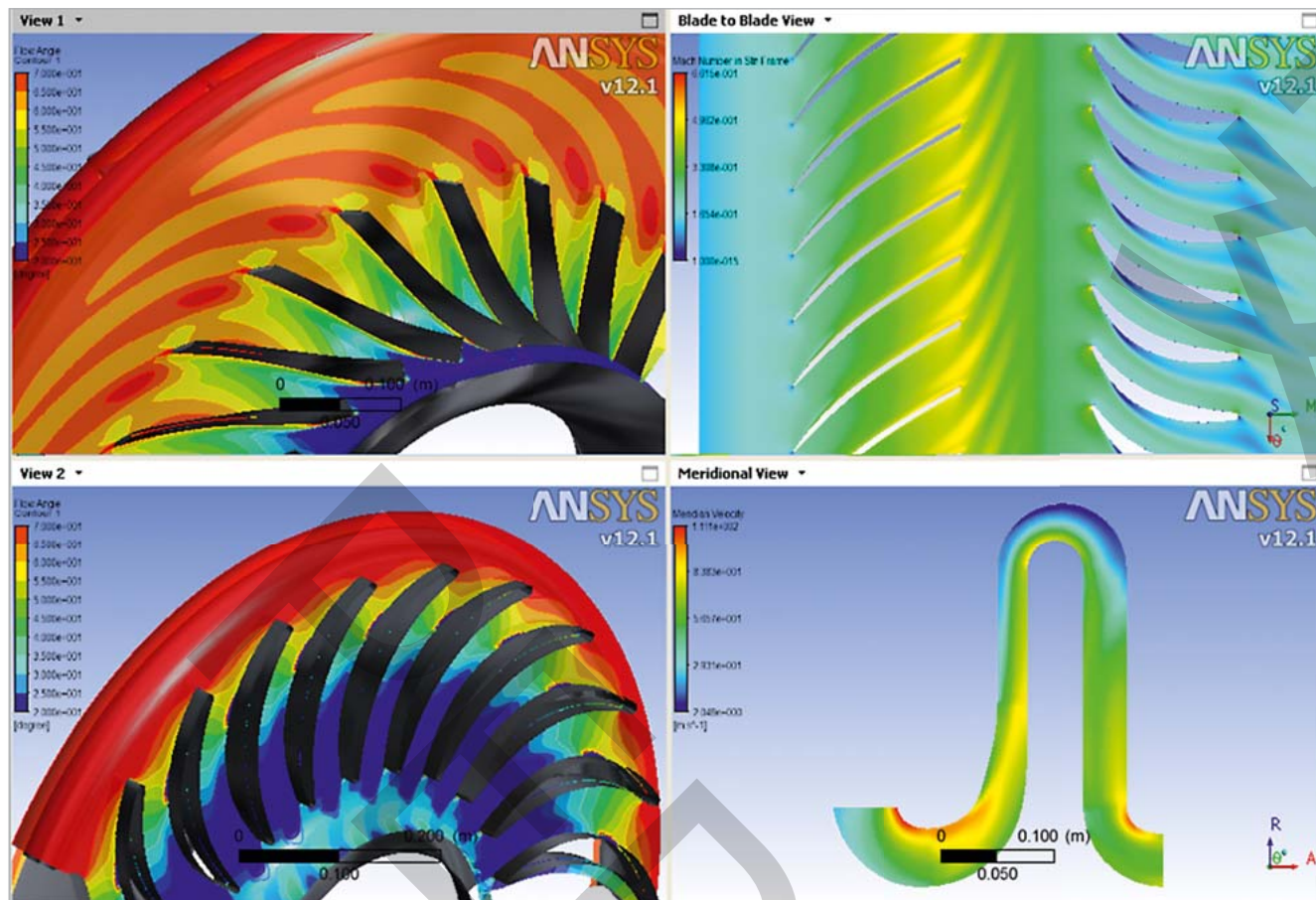


Fig. 2: CFD simulation results

### Computational fluid dynamics

A key advantage of the integrated approach is that both the flow and the structural groups work with the same design geometry within the ANSYS Workbench environment. This saves a considerable amount of time by eliminating the need for sending modifications back and forth to enter them into the model. The integration also includes the structural simulation, as well as the flow simulation, into the optimization process. Thus, for example, the optimization can be configured to select the design with the highest efficiency while also considering specific static and dynamic mechanical properties.

Based on the mesh resolution defined by the user, ANSYS TurboGrid was used to automatically generate the mesh for the computational fluid dynamics (CFD) simulation. The model included one passage per component with a profile-transformation rotor-stator interface as well as with chronological periodic interfaces. The total pressure and temperature were defined at the inlet, while the mass flow rate was defined at the outlet. Assuming an ideal gas, ANSYS CFX was then used to solve the model. The output parameters, such as total pressure, temperature ratio and isentropic or polytropic efficiency were determined using CFX-Post. Fig. 2 shows typical simulation results. The transient rotor-stator capability resolved the true transient interaction between components in regard to maximum accuracy. It can be applied to individ-

ual pairs of blade passages or to the entire 360-degree machine. Setup and use was as simple as it had been with the other frame-change models. It was also possible to combine transient and steady-state frame change interfaces in one computation. This was complemented by the inclusion of the second-order time differencing, which provided greater transient accuracy. Furthermore, transient blade row (Time- and Fourier transformation) models allowed unequal pitch systems to simulate multi-rows using only a few blade passages and less than the full 360-degree geometry.

### Structural analysis

The mechanical model used one segment of the rotor with cyclic symmetry reducing computational time without any loss of numerical accuracy. The model was fixed at the inner radius. The rotor was loaded by centrifugal force and fluid pressure using results of the CFD simulation. Data handling and fluid-structure coupling were automatically performed in ANSYS Workbench, as shown in Fig. 3. After the completion of the static simulation, a pre-stressed modal analysis was performed. The results of the mechanical simulation included the maximal displacement, von Mises stress and the eigenfrequencies. The design requirements included an upper limit of those stress and eigenvalues that did not match the rotational velocity in order to avoid resonance.

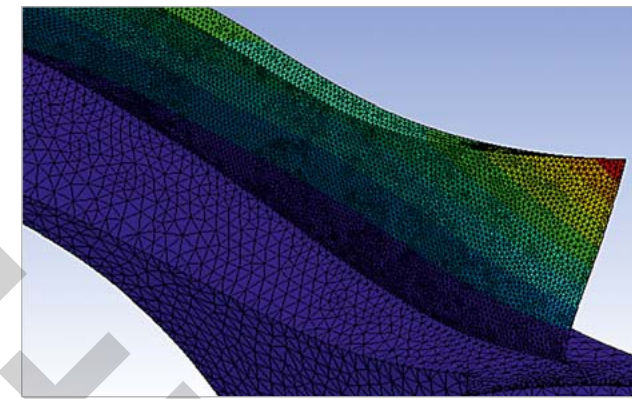


Fig. 3a: Mechanical displacement

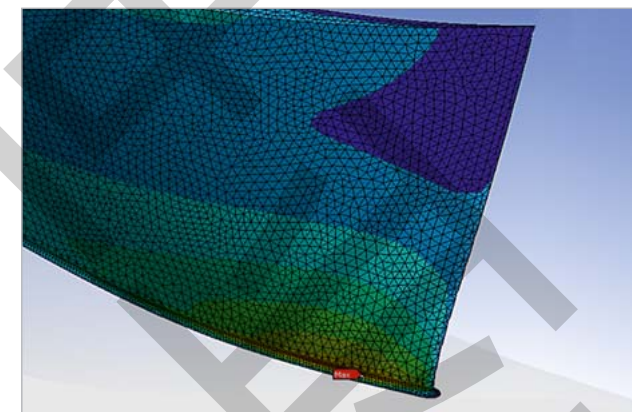


Fig. 3b: Mechanical stress

### Sensitivity analysis

With the flow and structural models set up, the next step was to automatically simulate the minimum number of design points needed to map out the complete design space. Thus, not only the design meeting the spec, but also those providing the highest possible level of performance while meeting other constraints, could be confidently identified. The software tool optiSlang was used for sensitivity analysis, optimization, robustness evaluation and reliability analysis. The optiSlang inside ANSYS Workbench integration runs simulations by importing parameters automatically, thus, no additional user input is required.

A sensitivity analysis uses a designed experiment to evaluate the reliability of the numerical model and identifies the most important input parameters. The Metamodel of Optimal Prognosis (MOP) algorithm uses Latin Hypercube Sampling to scan the multidimensional space of the input parameters. A Latin Hypercube is an n-dimensional object representing n different analyzed design parameters where each sample is the only one in its axis-aligned hyperplane. In this case, there were about 50 design parameters and about 100 design points were solved in order to create the MOP. This model represented the original physical problem and enables analyses of various design configurations without any further simulation runs.

The integration platform optiSlang inside ANSYS Workbench provides a seamless data transfer between applications and process controllers that sequentially simulate all of the design points and collate the outputs. Parametric persistence makes it possible to automate the optimization process including file transfer, mapping between physics, boundary conditions, etc. When the user clicks the Update All Design Points button, the first design point, containing the first set of parameter values, is sent to the parameter manager of ANSYS Workbench. There, the design modifications are processed from the CAD system to post-processing. The new design point is simulated and output results are passed to the design point table where they are stored. The process continues until all design points are solved and the design space is defined for later optimization.

optiSlang's Coefficient of Prognosis (CoP) determines whether the metamodel is reliable or not. This calculation also determines which input parameters have a strong influence on the outputs. The response surface graphically depicts the influence of the relevant parameters on the system's performance and shows where the highest efficiency is located. Fig. 4 shows the CoP and the response surface. In this case, the CoP was 84%, which indicated that the model was admissible but still could be optimized. The sensitivity analysis generated an efficiency of above 89% based on relatively rough simulations run parallel on a computing network overnight. This is about the maximum level that a highly experienced designer could expect to achieve within a reasonable time period.

The sensitivity analysis also showed that the eight most significant parameters account for nearly all result variations. This information was used to decisively reduce the time required for the detailed simulation by eliminating the

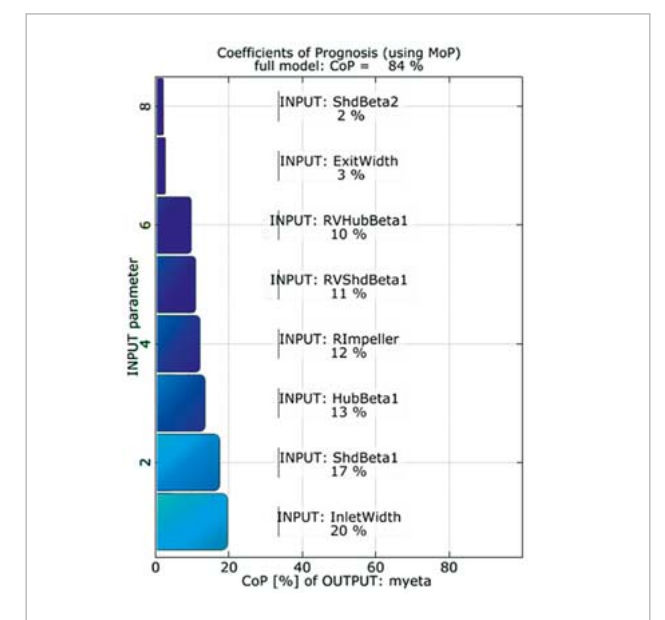


Fig. 4a: Coefficient of Prognosis (CoP)



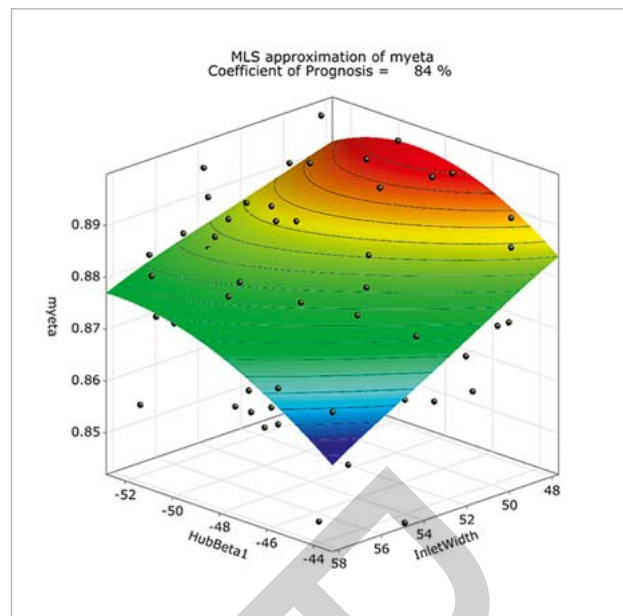


Fig. 4b: Response surface

variables that do not appear to have a significant impact on the results. For verification, the engineer can also check the numeric model, such as by examining the upper and lower bounds of the design parameters.

### Design optimization

With the entire design space examined and the most promising region selected, the next step was running a more detailed simulation. optiSLang's optimizer provides a wide selection of algorithms. In this case, the sensitivity analysis showed that the practical designs were located in a relatively small area of the design space. The Adaptive Response Surface Method (ARSM) was selected because of its efficiency to generate optimal solution based on starting points that are already in the vicinity of the optimum. If the sensitivity analysis had shown many design space areas containing practical designs, it would have been necessary to choose a different algorithm.

	Initial	SA	ARSM	EA
Pressure Ratio	1.3456	1.3497	1.3479	1.3485
Efficiency [%]	86.72	89.15	90.62	90.67
# Simulations	-	100	105	84

Table 1: design optimization

The direct optimization with ARSM generated another 1.5% improvement in the efficiency level to 90.62%, which is truly a best-in-class result. This level of efficiency is beyond what could be reached by using manual methods regardless of the designer's experience. With ARSM, approx. 10

simulations can be run parallel resulting in a required time of about three days. Using all parameters, a second optimization was performed with an Evolutionary Algorithm (EA) as a control point to check whether the elimination of design parameters in the first optimization was appropriate or not. The EA simulation hardly provided any further improvement, confirming that the additional input parameters have a negligible effect on the results.

### Robustness evaluation

So far, the simulation dealt with an idealized setting where, according to the CAD geometry for example a 50 degrees angle is assumed to be exactly 50 degrees. In real world manufacturing, of course, one blade will have an angle of 50.1, the next 49.9 and so on. All of the other design parameters, including material properties, also vary. In order to determine the effect of this variance, we need to design a probability distribution that will simulate the real world manufacturing output. A Gaussian distribution is often used to model manufacturing tolerances while a log normal or Weibull distribution is common for material properties. Again, a Latin Hypercube sampling distribution was used because of its efficient ability to estimate the outputs of a large number of possible designs based on a small sample of actual simulations.

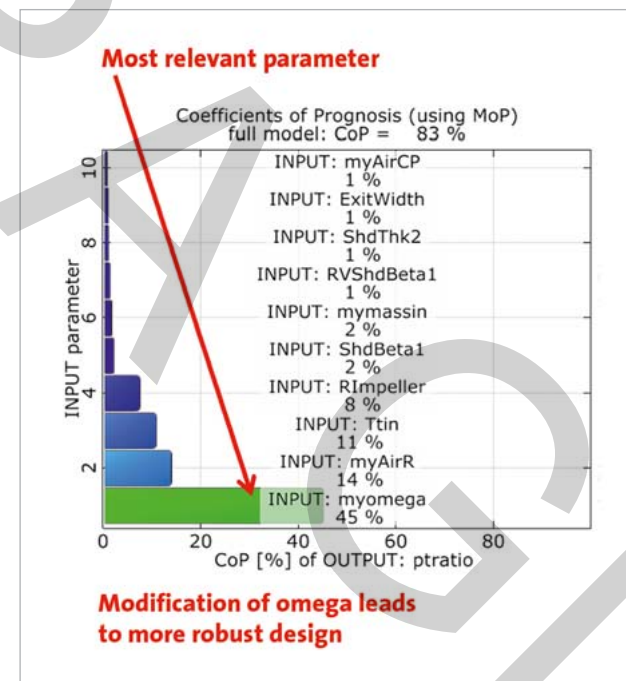


Fig. 5a: CoP of myomega variable

The robustness analysis results showed that an estimated 13% of the manufacturing volume had a pressure ratio outside the limits. The CoP was 83 percent, which indicated that the results are reliable. The robustness analysis indicated that the fluctuation of pressure was primarily caused by the rotational velocity, the so called myomega variable

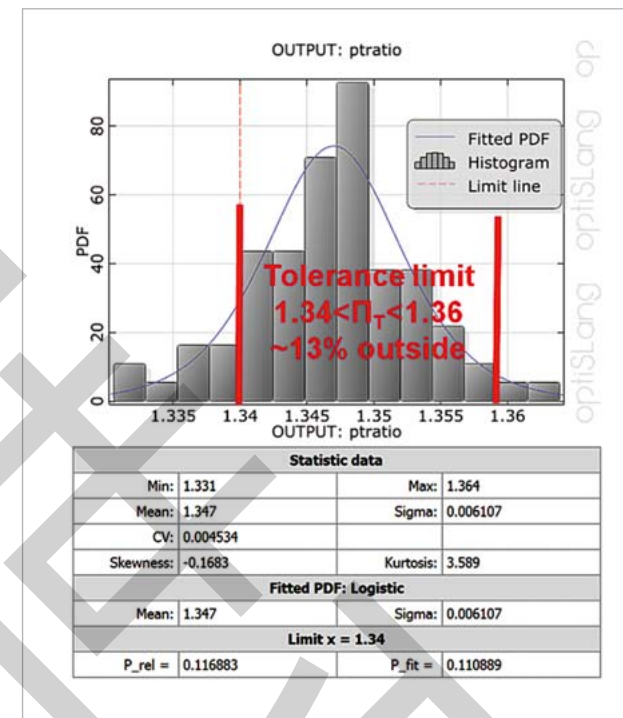


Fig. 5b: Robustness evaluation of pressure ratio

shown in Fig. 5. Controlling this parameter will have a major impact on pressure distribution. It was also worth noting that the pressure ratio was tilted towards the lower limit. Shifting the distribution in the direction of the higher limit will significantly reduce the proportion outside the limits. The other design parameters caused negligible effects which means there might be potential for opening up manufacturing tolerances in order to reduce costs.

### Conclusion

By using the multi-physics platforms ANSYS Workbench and optiSLang, an automated process can be applied to achieve robust design optimization with reproducible methods. The process provides automatic geometry regeneration, high-quality meshing for each possible design, automatic solver execution as well as automatic post-processing. Robust design optimization makes the virtual development process more sophisticated, for example by including the impact of manufacturing variations. The results can be seen in improved product performance and Robustness.

Author // Johannes Einzinger (ANSYS Germany GmbH)

Source // [www.dynardo.de/en/library](http://www.dynardo.de/en/library)

## DYNARDO TRAININGS

At our trainings, we provide basic or expert knowledge of our software products and inform you about methods and current issues in the CAE sector.

### Info Days and Webinars

During our info days and webinars, you will receive an introduction to performing complex, non-linear FE-calculations using optiSLang, multiPlas, SoS and ETK. At regular webinars, you can easily get information about all relevant issues of CAE-based optimization and stochastic analysis. During an information day, you will additionally have the opportunity to discuss your specific optimization task with our experts and develop first approaches to solutions.

### Trainings

For a competent and customized introduction to our software products, visit our basic or expert trainings clearly explaining theory and application of a sensitivity analysis, multidisciplinary optimization and robustness evaluation. The trainings are not only for engineers, but are also perfectly suited for decision makers in the CAE-based simulation field. For all trainings there is a discount of 50% for students and 30% for university members/PHDs.

### Info

You will find all information as well as an overview of the current training program at:

[www.dynardo.de/en/trainings](http://www.dynardo.de/en/trainings)



## HIGH FREQUENCY SIMULATION

ANSYS and optiSLang were applied to optimize the geometry of different antenna types concerning resonance, interference and impedance behavior.

High frequency electromagnetics is concerned with the propagation of waves. In free space, electromagnetic excitations propagate with 300,000 km/s, the speed of light. For this reason, a specific wave length can be associated with a certain electromagnetic wave of a given frequency. For example, in a vacuum, the wave length at 1 GHz is 30 cm. Wave phenomena are only relevant if the considered structure has a size which is comparable to the wave length. For typical radio frequency (RF) applications, this implies that high frequency starts at the MHz to GHz range.

There are many high frequency applications in daily life. Most of them are concerned with the transfer and processing of information. However, there are also applications in radar technology, in medical imaging applications, as well as in microwave heating.

### Field and circuit simulation

Electromagnetic waves, like radio waves, can propagate freely in space. But they can also be bound to conductors or waveguides as in coaxial cables or on micro strip lines. An antenna is a passive device that converts guided into free waves or

vice versa. However, in the designing process of printed circuit boards or connectors, the goal is to prevent the signal from scattering off imperfections which would cause undesirable effects like reflections, cross talk or radiated emissions. In order to deal with such issues, ANSYS developed the Electromagnetics Suite containing industry standard field and circuit simulators. In this article, a special focus is placed on ANSYS HFSS as an all-purpose, three dimensional high frequency field simulator. This fully parametric simulation environment combined with automatic adaptive meshing can be used for robust design optimization of RF systems. The adaptive meshing process ensures the desired solution accuracy for any required result, like impedances or scattering parameters. In this way Ansys HFSS eliminates numerical noise due to the meshing process.

### Most RF applications use effects like resonance, interference and matching of impedances as functioning principles:

1. For example, an antenna operating at resonance generates large currents on its structure while it is driven with a small input signal. The large currents produce electromagnetic fields which propagate into free space. The resonance on the antenna can also be seen as a stand-

ing wave. On a dipole antenna, the wave length of the standing wave is twice the length of the dipole. This describes the relation between the size of the antenna and the frequency of operation.

2. In the case of a microwave cavity filter, all three principles can be clearly observed. The filter has to have the appropriate number of resonances in the pass band. The coupling impedances between the different cavity resonators have to be chosen appropriately, as predicted, in the ideal prototype filter. The structure of pass- and stop bands is due to constructive and destructive interferences between the reflected and transmitted waves of the different cavities.

As demonstrated above, the scattering parameters (S-parameters) and impedances represent important values to quantify the functioning principles mentioned above. They also can be used for a robust design optimization of RF components.

### Examples

#### Optimization of a dual band antenna

A dual band antenna works at two frequency bands. In Fig. 1, the geometry of a dual band slot antenna is shown. The return loss (see Fig. 2 top) of the initial design already had two resonances with one close to 2.4GHz and the other close to 5.8GHz. However, the first value was not at the right position and was very sharp. The second minima at -12dB shows a rather poor matching performance. To improve the design, an optimization using optiSLang was conducted. Afterwards, both minima were in the right position, well below -15dB (see Fig. 2 bottom) and also showed an extended bandwidth. The production of printed antennas involves many uncertainties concerning the electric material properties of substrates, like FR4 and, of course, there are tolerances in the process of fabricating a printed circuit board (PCB). A robustness analysis of the design using optiSLang quantifies the maximum allowed tolerances and provides a profound understanding useful for appropriate decision making concerning cost versus accuracy issues and material quality management.

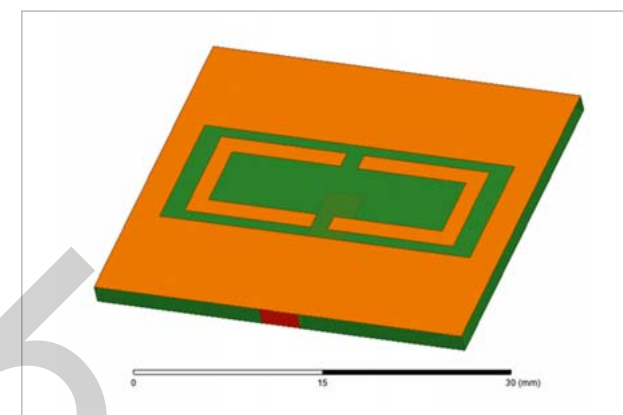


Fig. 1: Geometry of a dual band slot antenna

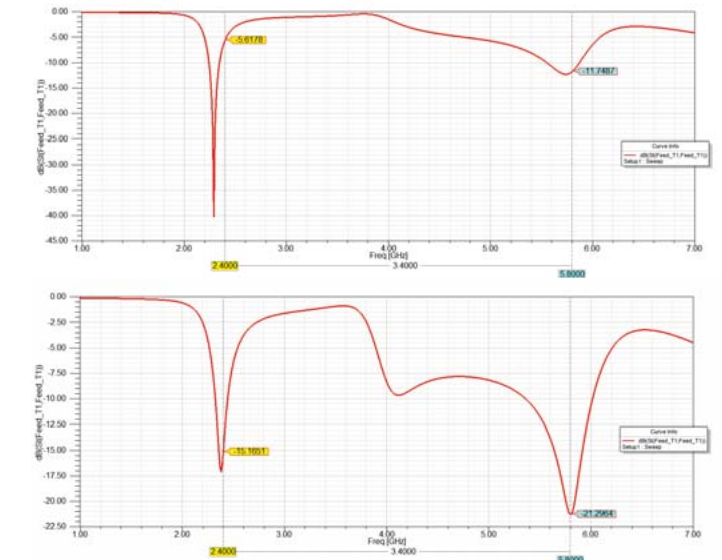


Fig. 2: Return loss of initial design (top) and optimized design (bottom)

#### Return loss optimization of a 2x2 antenna array

In cooperation with the Austrian antenna manufacturer PIDSO, a 2x2 antenna array was analyzed (Fig. 3), which is used for high-gain, line-of-sight data transmission towards moving objects (tracking). In order to track objects, the antenna array was installed on a gimbal assembly. A four-port hybrid coupler was integrated for transforming four output signals into composite ones for signal transmission as well as differential ones for tracking. An incident wave that is received at an angle by the antenna array causes phase-shifted signals at the patch antennas. Here, the hybrid coupler should use constructive and destructive interference to generate sum and differential signals. The edge length of the hybrid coupler is approximately a quarter wave length. The S-matrix for the transmission behavior of the coupler from input to output ports has to satisfy the following relation describing the interference.

$$S_{Out,In} \sim \begin{pmatrix} i & 1 & i & 1 \\ 1 & i & 1 & i \\ -i & 1 & i & -1 \\ -1 & i & 1 & -i \end{pmatrix}$$

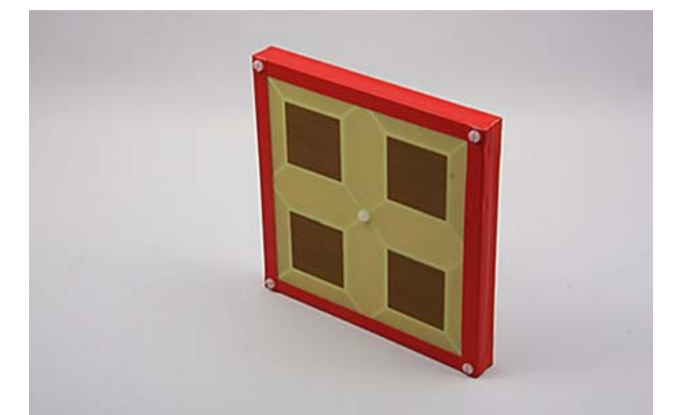


Fig. 3: The antenna array is used for directional data transmission



To adapt the coupler to a given frequency, the geometry had to be parameterized. Due to the geometry's symmetry, five edge lengths, one angle as well as the position of the parallelogram in regard to the rectangles, were considered (Fig. 4). The field simulation of the parameterized structure at the given frequency was performed with ANSYS HFSS. The aim of the optimization using optiSlang was to minimize the mean square deviation between the real coupler S-matrix and the ideal one adapted by a corresponding multiplicative (complex) constant. Moreover, the return loss of the sum port should be less than -12dB. The sensitivity analysis using optiSlang revealed that six of the seven parameters have significant influence on the two target parameters. An optimization applying an adaptive response surface method resulted in a sufficient geometry af-

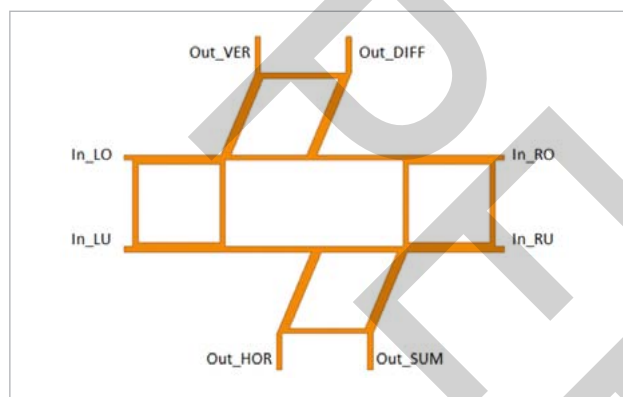


Fig. 4: The edges of the hybrid coupler are approx. one-quarter wavelength

ter running an overnight computation. The plot (Fig. 5) of the output signals at the sum port as well as at the horizontal and vertical differential ports show the high optimization quality. The contours of horizontal and vertical differential signals form a rectangular coordinate system across a large angular range. It additionally indicates that the sum signal hardly depends on the phase differences. Fig. 6 shows the electric field strength distribution displaying that there is hardly any reception at the differential ports of the hybrid coupler if the waves arrive orthogonal at the antenna patches. A further step towards the entire design of the antenna is the connection of the hybrid coupler to the antenna array via a microstrip line. For this purpose, a circuit simulation is conducted with ANSYS designer. Here, for example, the difference in length of the microstrip lines and the stub capacity for feed tuning of the patch antennas could be used as input parameters. Then, the gain plot of the antenna assembly can be simulated and optimized via the dynamic link between ANSYS designer and HFSS.

Finally, after reassembling the entire antenna, a field simulation had to be conducted (Fig. 7). The necessary geometry was derived from the result of the circuit simulation. By this approach, the design process was accelerated significantly. In further steps, ANSYS combined with optiSlang also allowed to analyze the robustness of designs exposed to other physical influences.

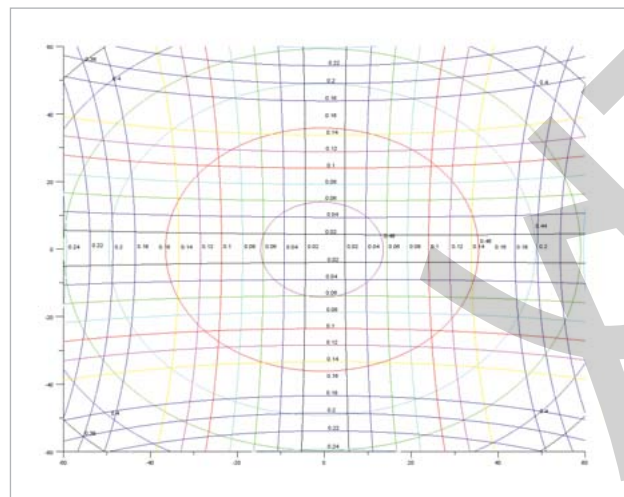


Fig. 5: The contour plot indicates the high quality of the optimization

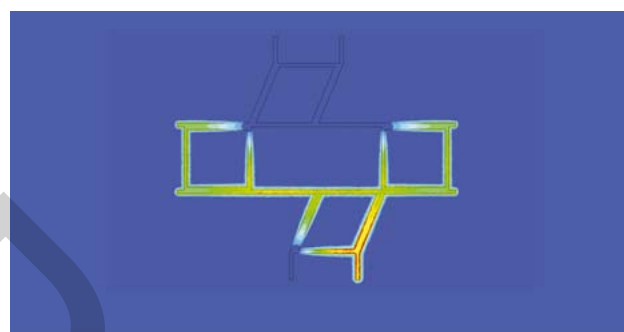


Fig. 6: The signals emitted from the antenna patches hardly reach the differential ports

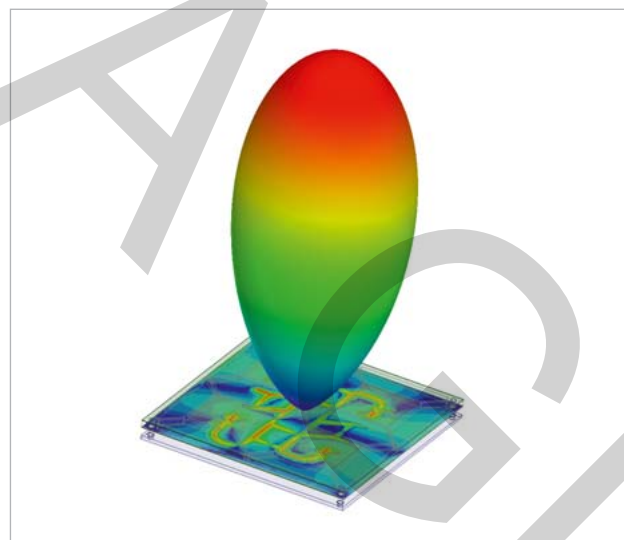


Fig. 7: Field simulation of the entirely assembled antenna

**Author //** Christian Römelsberger (CADFEM GmbH)

**PIDSO**  
Propagation Ideas & Solutions

**Contact PIDSO GmbH //** Lastenstrasse 19, A-1230 Wien  
Tel. +43 (0) 1 25 24 189, [www.pidso.com](http://www.pidso.com)

## ANNUAL WEIMAR OPTIMIZATION AND STOCHASTIC DAYS

Your conference for CAE-based parametric optimization, stochastic analysis and Robust Design Optimization in virtual product development.

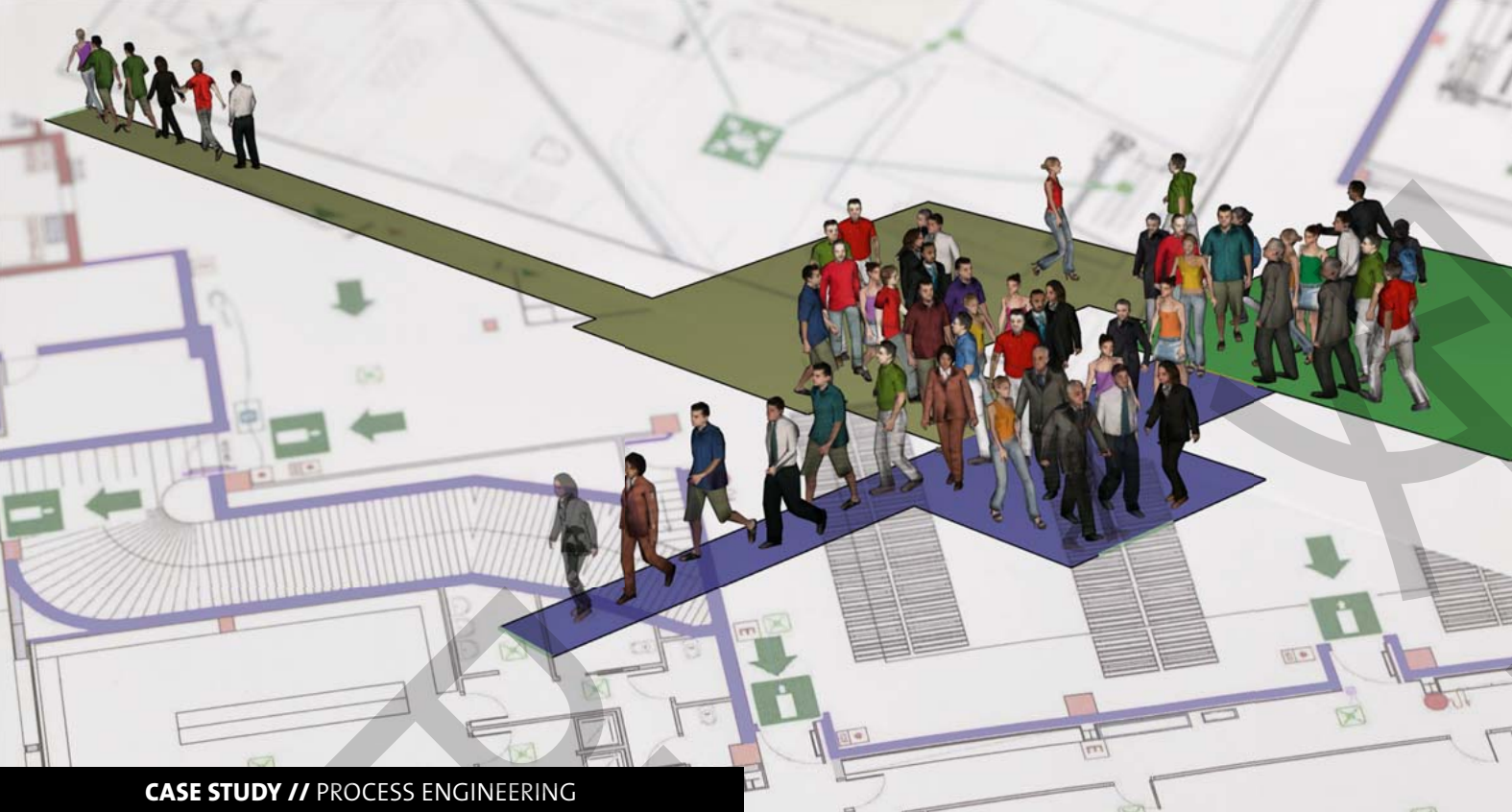
The annual conference aims at promoting successful applications of parametric optimization and CAE-based stochastic analysis in virtual product design. The conference offers focused information and training in practical seminars and interdisciplinary lectures. Users can talk about their experiences in parametric optimization, service providers present their new developments and scientific research institutions inform about state-of-the-art RDO methodology.

Take the opportunity to obtain and exchange knowledge with recognized experts from science and industry.

You will find more information and current dates at:  
[www.dynardo.de/en/wosd](http://www.dynardo.de/en/wosd).

We are looking forward to welcoming you to the next Weimar Optimization and Stochastic Days.





CASE STUDY // PROCESS ENGINEERING

## SENSITIVITY ANALYSIS OF EVACUATION SIMULATIONS

Simulation of evacuations is an efficient way to find the best escape concepts and to increase the safety of buildings. The importance of different input parameters for the result is investigated by stochastic sensitivity analyses and evaluated by the Model of Optimal Prognosis (MOP).

### Introduction

Safe evacuation of persons from buildings in cases of fire or other emergency situations is getting an increasing public attention. There are many sad examples in history where inadequate escape routes in the case of fire have caused the death of many people. The “Iroquois Theatre Fire” in Chicago with about 605 victims or the “Karlslust Dance Hall Fire” in Berlin with about 88 victims are only two examples. By evacuation simulations it is possible to discover critical parts of escape concepts in order to optimize the safety of buildings.

As evacuation simulation is a relatively young discipline, there is a strong need to develop knowledge and expertise on the sensitivity of the results on statistic or deterministic variation of input parameters. The probability distributions of most input parameters are not sufficiently known. To find out for which of them it is worth to carry out detailed investigations and experiments, probabilistic sensitivity studies are an efficient method. Typical simulation times are very short, even for big models – for less than 1000 occupants often below one minute. From the cost point of view, this makes evacuation simulation an ideal application area for stochastic methods where high numbers of samples are needed to find reliable results.

Evacuation simulation models are employed to simulate crowd movement in emergency situations. These models can be divided into four different groups: flow-based models, cellular automata, agent-based and activity-based models.

The sensitivity study was carried out with Pathfinder and optiSLang. Pathfinder is an agent-based model that individualises the movement of groups. Every evacuee is defined by a set of attributes like for example walking speed, shoulder width or comfort distance.

### Numerical Model of Evacuation

#### Input Parameters

Whether an escape route is considered safe or not strongly depends on the amount of people using it in case of an emergency. The capacity of every section of a path is limited by its length and width as well as by obstructions and restrictions (doors) along its way. The movement of the crowd depends on physical factors like the area occupied by the bodies and the density of the group. The behaviour

of the crowd also depends on many other properties of the individuals in the group like, for example, prior knowledge, knowledge of the place and leadership behaviour.

Pathfinder offers two modes of occupant movement: SFPE mode and steering mode. This study was made using the steering mode. The steering system in Pathfinder moves occupants so that they roughly follow their current seek curve and can respond to a changing environment.

#### Geometry

In Pathfinder, floors are divided into an irregular triangular navigation mesh. The mesh can be divided in multiple rooms on multiple floors in 3D. Floors with different heights can be connected by stairs, ramps or elevators. Occupants can only move on the navigation mesh while obstacles, like furniture or closed interior rooms, are simply represented by holes in the navigation mesh.

#### Solution Procedure

The numerical solution to determine occupant movements is discretised in time and uses an explicit integration scheme. In each time step the following procedure is carried out:

1. **Update targets:** Determine the current target for each occupant, taking into account different exits and individual properties and plan a path to reach the target.
2. **Calculate the movement of occupants** by explicit Euler integration, taking into account the current velocity of each occupant and individual acceleration to normal walking speed at start of the simulation and after passing obstacles.
3. **Modify escape paths** in order to account for other occupants who represent dynamic obstacles in their way and allow decisions for other exits and paths according to the local situation.

#### Path Generation

Escape paths along the navigation mesh are defined by a search algorithm along points on the edges of the mesh triangles. As there are often different paths on which a destination can be reached, a decision needs to be made on the most appropriate one. The solution algorithm selects the “locally quickest” path to the final destination. For this decision, it is assumed that the occupant knows about the doors in the local room and the queues at those doors as well as the distances to them. This evaluation is made by help of a weighted cost function of four steering behaviours (seek, separate, avoid walls and avoid occupants). Having determined the lowest cost direction, the maximum distance that should be travelled along this direction will be calculated. As the occupant moves, he has to account for dynamic obstacles like other occupants and, therefore, has to adjust his way by idling or seeking. Depending on the state and speed of the occupant, different sample directions are tested.

### Sensitivity Analysis

Three sensitivity studies were carried out, each with a different objective:

1. Determine which of the parameters describing occupant properties are most important. For this purpose, a study with constant geometric parameters was made.
2. Investigate the influence of different geometric parameters. In this study, occupant properties are constant.
3. Evaluate the importance of geometric parameters versus occupant properties. In this study, all input parameters are varied stochastically.

#### Input and output parameters

Input parameters are divided into two groups: occupant properties and room geometry (Table 1 and 2).

Input Parameter	Unit	min	max
accelFactor	s	0.50	1.10
radius	m	0.14	0.25
maxVel	m/s	0.36	1.58
reactTime	s	0.09	0.11
minSqueezeFactor	-	0.50	1.00
persistTime	s	0.50	1.50
collisionResponseTime	s	0.50	2.00
comfortDist	m	0.00	0.50
slowFactor	-	0.05	0.15
localQueueTimeFactor	-	0.80	1.00
localTravelTimeFactor	-	0.80	1.00
tailTimeFactor	-	0.80	1.00

Table 1: Input parameters for occupant properties

Input Parameter	Unit	min	max
exit_west	m	1.00	1.40
exit_south	m	1.00	1.40
exit_east	m	1.00	1.40
door1	m	1.00	1.80
door2	m	1.00	1.80
door3	m	1.00	1.80

Table 2: Input parameters for room geometry

Parameters in Table 1 are assumed to have a normal probability distribution. Input parameters for the room geometry are shown in Table 2. They describe the width of the interior doors and emergency exits (see Fig. 1 next page). Parameters in Table 2 are assumed to have a uniform probability distribution. The input parameters of the occupants vary in ranges that correspond to typical properties of healthy people. The maximum speed of an occupant, for example, varies in a range



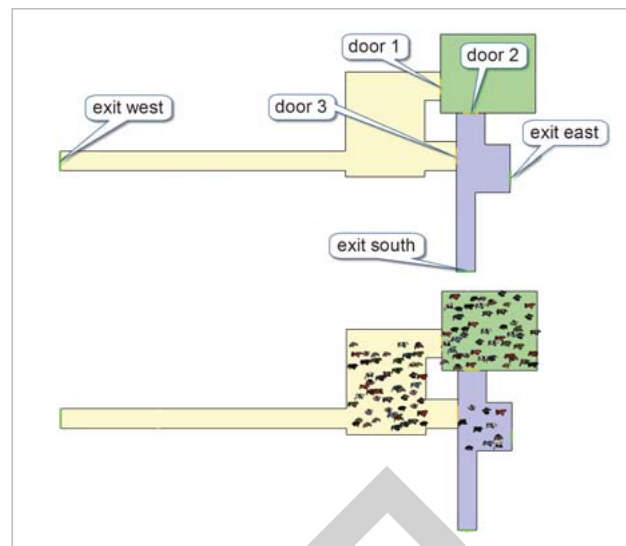


Fig. 1: Room geometry (top) and initial distribution of occupants (bottom)

that is typical for people who can move without mobility aids like crutches, walkers or wheel chairs. The input parameters for occupant properties are shown in Table 1. The most important ones are:

- Radius: radius of the moving cylinder by which occupants are represented. Its range corresponds to the range of human shoulder width
- Maximum velocity (maxVel): maximum velocity at which an occupant can move
- Comfort distance (comfort\_Dist): specifies the desired distance one occupant will try to maintain with others nearby such as when waiting in queues
- Collision Response Time: when multiplied by an occupant's current speed, this parameter controls the distance at which an occupant will start recording a cost for colliding with other occupants when steering,
- Acceleration time (accel\_Factor): specifies the amount of time it takes for the occupant to reach maximum speed from rest or to reach rest from maximum speed.

The most important output parameter for evacuation simulations is the time until the last evacuee has left the building. This evacuation time (maxTime) is measured in seconds. Other output parameters that evaluate the distribution of occupants to the different exits and the flow through the exits could be important for a subsequent optimization based on the sensitivity results.

### Room Geometry

The fictive room geometry was set up with the objective to provoke changes of the "locally quickest" path during the simulation. There are multiple ways with similar length to the exits. The building has a total area of 110 m<sup>2</sup> consisting of three rooms on one floor connected by three doors with one long corridor and 3 exits. 110 occupants were chosen for escape scenario.

### Sampling method

For all analyses, optiSlang's Advanced Latin Hypercube Sampling was applied to generate 500 or 1000 stochastic samples. The results were evaluated after calculation of the Metamodel of Optimal Prognosis (MOP) that allows to assess the quality of prognosis for the simulation model and is used to characterise the influence of each input parameter on each output parameter by evaluation of their ability to predict results. Simulation time for 500 samples was 35 min on an office PC with 4-core-CPU.

### Study 1: Sensitivity to Occupant Properties

In this study, only occupant properties were used as stochastically varying input parameters. All geometric parameters of the building were held constant. The result shows that walking speed (maxVel) and outer dimensions (radius) of the occupants have highest influence on the evacuation time. Further, the acceleration time (accel\_Factor) and the comfort distance (comfort\_Dist) are important for the result.

The graph in Fig. 2 shows the Coefficients of Prognosis (CoP). The CoPs are calculated with the MOP. This metamodel is based on the results of the sensitivity analysis and uses approximation algorithms to provide a response surface which is applied to evaluate the quality of prognoses that can be made with the simulation model. The results in Fig. 2 read as follows: 54% of the variations in the results of the output parameter maxTime (evacuation time) can be explained by the variations of the input parameter maxVel (maximum velocity of an occupant). Input parameters with contribution of <1% are not displayed in this graph. The CoP is an appropriate measure to evaluate the quality of a model. Low CoP values are generally an indicator of an error in the model, for example, due to input errors committed by the user or in the simulation software. In this example, a high CoP of 96% was calculated.

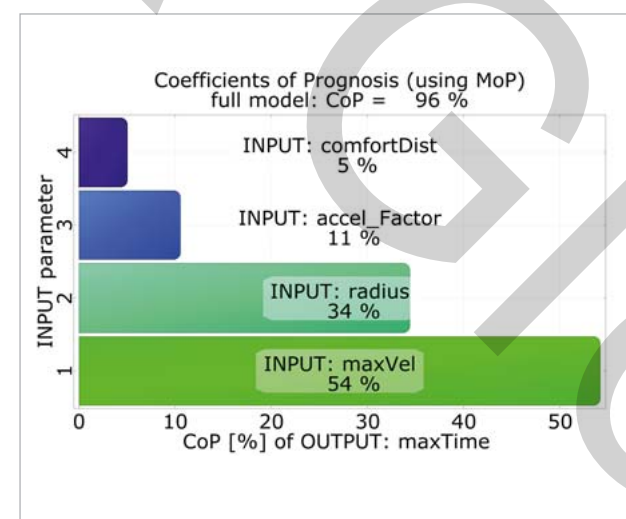


Fig. 2: Study 1 (only properties of occupants vary), Coefficients of Prognosis for evacuation time (maxTime)

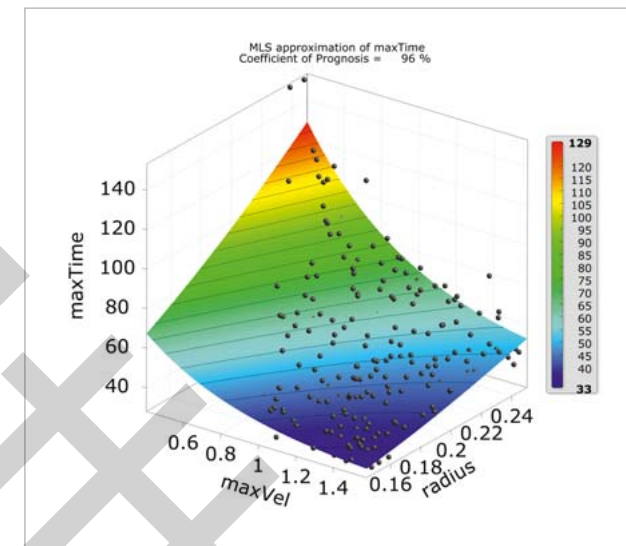


Fig. 3: Study 1 (only properties of occupants vary), 3D response surface for evacuation time (MOP)

### Study 2: Sensitivity to Geometric Parameters

In real projects, a typical task for evacuation simulations is, for example, to prove that replacement of existing doors against wider ones is not required because safe egress is possible without expensive modifications. In study 2 of the investigated example, the interior door 3 has the highest importance: 32% of the variation of the evacuation time can be explained by the variations of the width of this door. This result is interesting because this door is not an emergency exit and therefore not considered to have such high importance for the result. Because of the queue at door 2 many occupants decide to take the second rescue path through door 1 (Fig. 4). But instead of following the crowd to the exit west (green arrow) they decide to take the "shortcut" through door 3 to the exit east (blue dotted arrow). To avoid this bottle-neck situation, escape route signs at door 3 have to show to exit west and not to door 3.

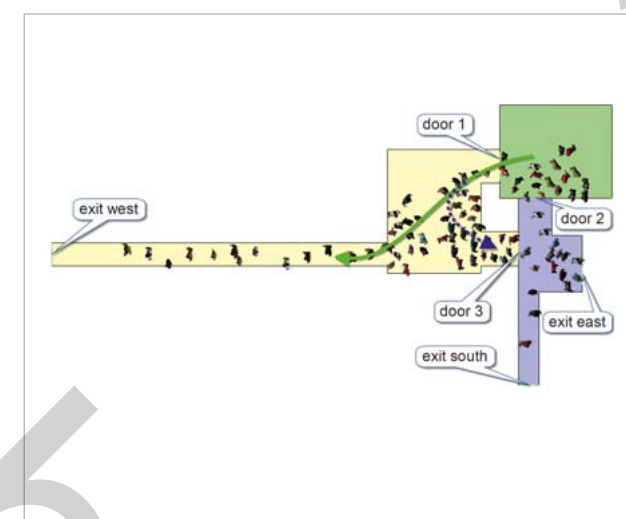


Fig. 4: Simulation sample of study 2, illustrating the importance of door 3

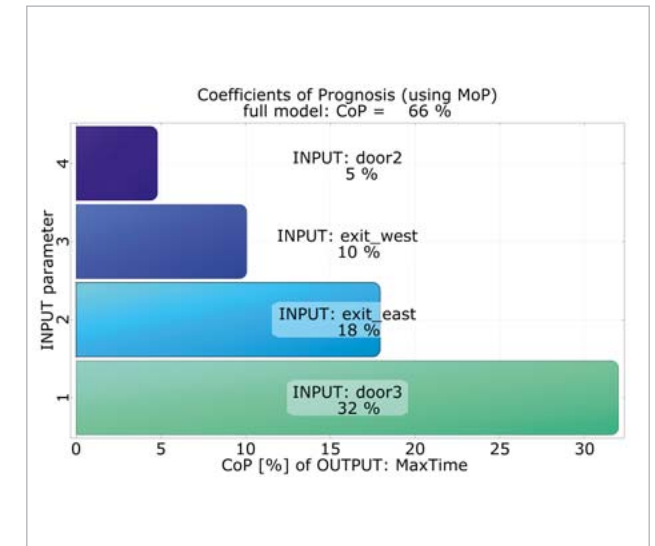


Fig. 5: Study 2 (only geometric parameters vary), Coefficients of Prognosis

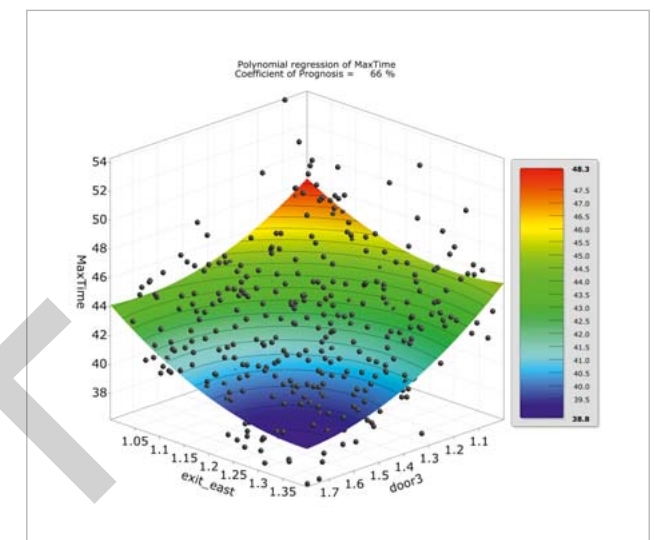


Fig. 6: Study 2 (only geometric parameters vary), 3D response surface, door 3 and exit east vs. evacuation time (MOP)

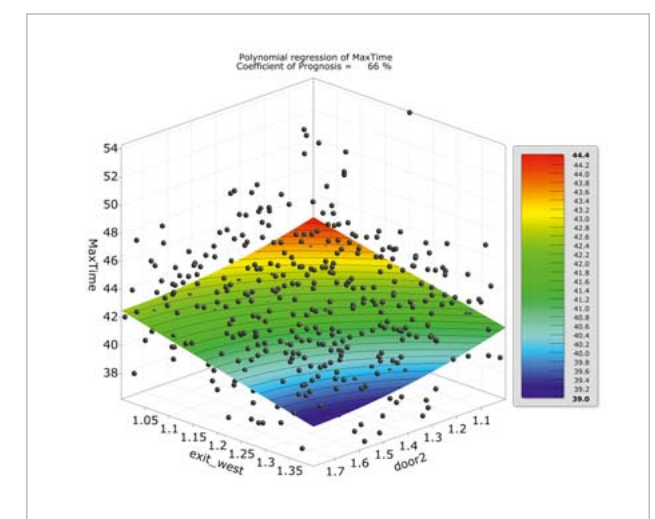


Fig. 7: Study 2: (only geometric parameters vary), 3D response surface, door 2 and exit west vs. evacuation time (MOP)



### Study 3: Relationship of Sensitivities to Geometric Parameters and Occupant Properties

In this study, both groups of input parameters – occupant properties and room geometry – are varied. As in study 1 and 2, the probability distribution of geometric parameters is uniform, whereas the occupant properties follow a normal distribution. An interesting result is that the occupant properties radius, maximum velocity and acceleration time are much more important for the evacuation time than the width of interior doors and emergency exits in this example (Fig. 9).

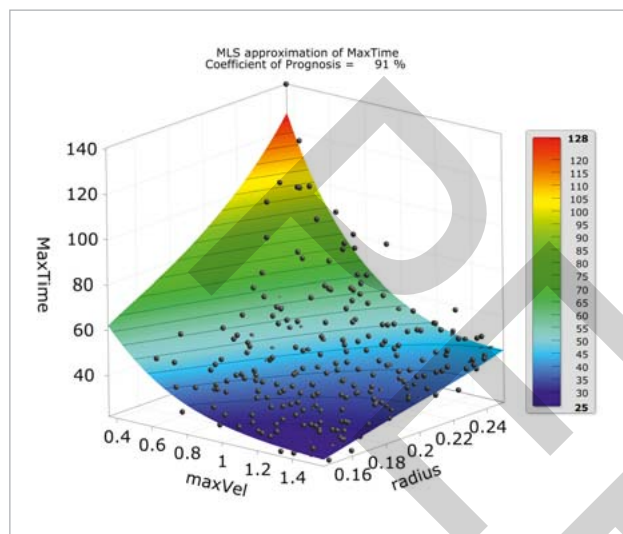


Fig. 8: Study 3 (Geometric Parameters and Occupant Properties vary), 3D response surface for evacuation time (MOP)

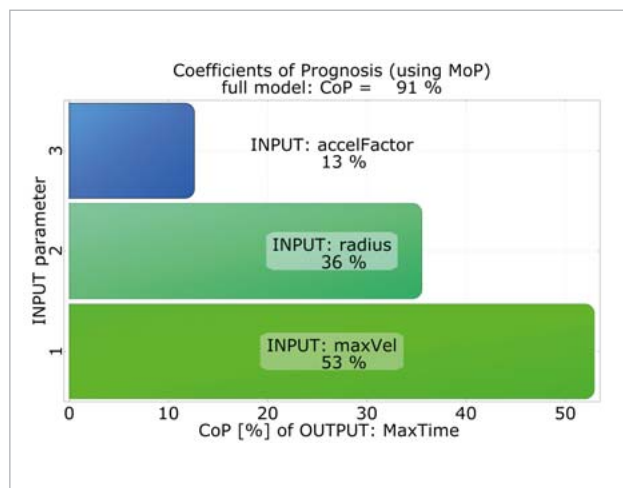


Fig. 9: Study 3 (Geometric Parameters and Occupant Properties vary), Coefficients of Prognosis

### Conclusions

By stochastic sensitivity analyses of evacuation simulations with an example building consisting of three connected rooms with 3 emergency exits it could be shown that:

- Only a few input parameters that describe occupant properties have significant influence on the evacuation time, mainly the radius and the walking speed are important.

- If both geometric and occupant parameters are varied, the variation of occupant parameters has bigger influence on the variation of results.

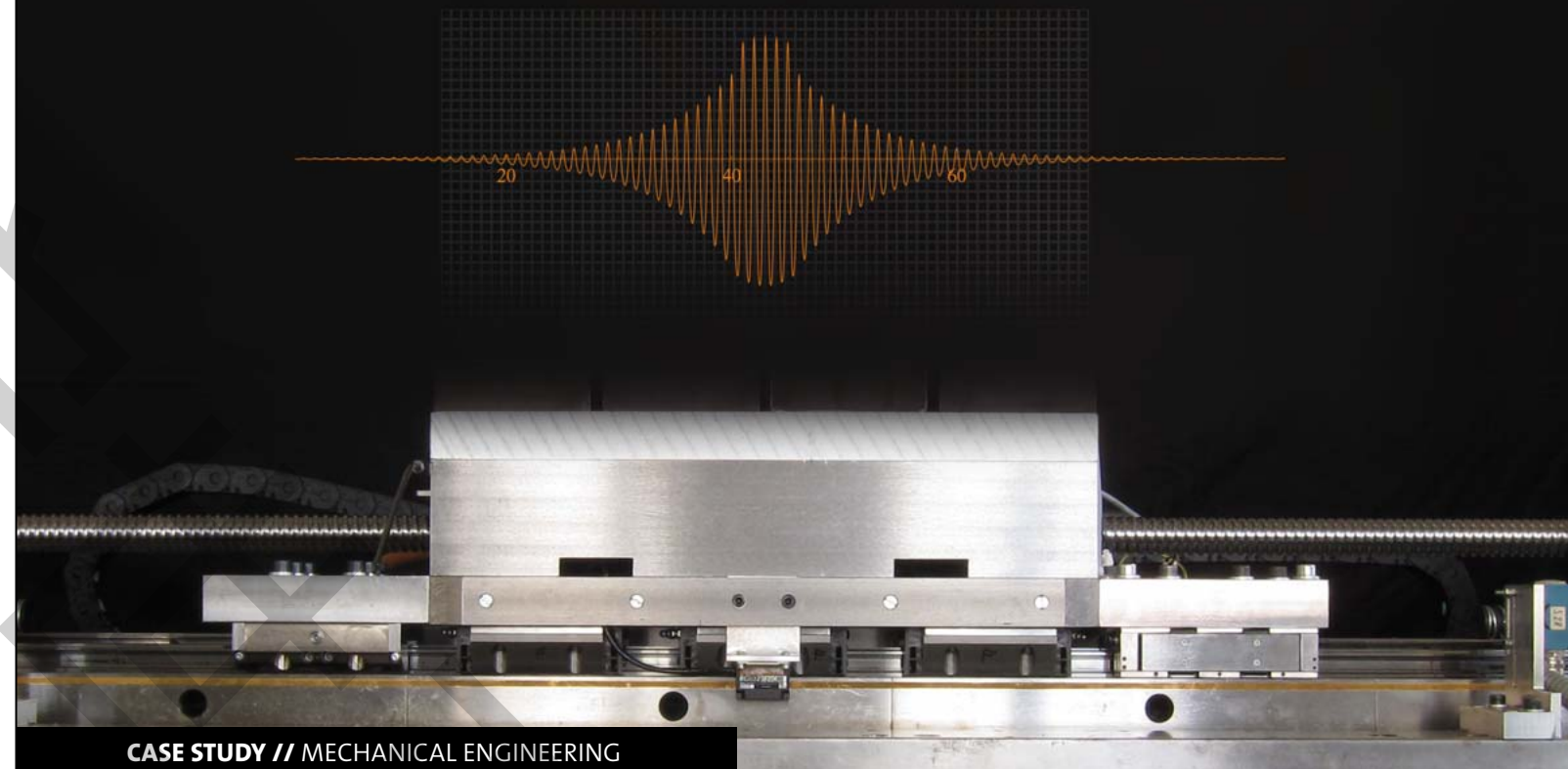
The percentage of people who walk at reduced speed and also require more floor space is increasing due to the current trend of an aging population. The results show that the presence of people with physical impairments who are using walking frames or other mobility aids among the evacuees would have a strong influence on the entire evacuation process and not only on the total evacuation time.

The results can be applied to increase the reliability of simulations by more precise determination of the most important input parameters. It is recommended to verify particularly the input data for occupant shoulder width, maximum walking speed and acceleration time.

The results were produced by use of one arbitrary example for the basic geometry. Further investigations should be made to find out if this result is valid on other geometries as well. Simulation-based optimization and robust design analysis can follow the sensitivity analyses to improve designs for evacuation.

**Authors //** Dr. Gerald Grewolls (SIMTEGO GmbH) / Prof. Dr. Kathrin Grewolls (Ingenieurbüro für Brandschutz Grewolls)

**Source //** [www.dynardo.de/en/library](http://www.dynardo.de/en/library)



### CASE STUDY // MECHANICAL ENGINEERING

## MODEL-BASED PARAMETER IDENTIFICATION: CAUSE AND EFFECT

**Model-based condition monitoring with ANSYS and optiSLang enables an understanding of correlations between the properties of individual components and their effects on the behavior of a machine.**

To assure acceptable machining tolerances and the quality of work pieces in the long run, it is necessary to monitor machine tools during the operating mode. Basically, there are three different strategies which can be categorized as “run to break”, “time-based preventive maintenance” and “condition-based maintenance”. The objective of the last approach is the permanent analysis of component properties during the period of operation.

In most cases, condition monitoring is based on the analysis of the vibration amplitudes measured by external acceleration sensors at various spots of the machine. This project presents a new approach that determines the physical characteristics of individual machine components based on the analysis of the machine vibration and system model.

The generation of an appropriate algorithm for the condition monitoring of a particular system requires a comprehensive knowledge of potential failure modes. In the case of a spindle nut drive, the abrasion of the runway is the most common problem. The erosion of the runway profile impairs the tribological properties of the contact surface and, as a consequence, reduces the prestress between balls,

nut and spindle. Furthermore, the loss of prestress reduces the total stiffness of the feed drive system causing a change of the system's eigenfrequencies. Therefore, an analysis of the eigenfrequencies of the feed drive can lead to determination of the stiffness in different subcomponents.

### Analysis using a simplified model

During the SIOCS project “Simulation-based parameter identification for online condition monitoring of a ball screw” at the ISW (Institute for Control Engineering of Machine Tools and Manufacturing Units) of Stuttgart University, calculations of the eigenfrequencies and the following analysis of the component stiffness were conducted by using a FE (Finite Element) model of a ball screw. In the first phase, a simplified 2-D FE model (Fig. 1, see next page) was developed with less than 50 degrees of freedom. The first eigenfrequency corresponded to the axial vibration of the axis and the second one characterized the torsional vibration of the spindle. Besides the table mass and the motor inertia, the simplified model also included the stiffness and damping parameters of nut, bearing and coupling. The correlation between the stiffness values and the first two cal-



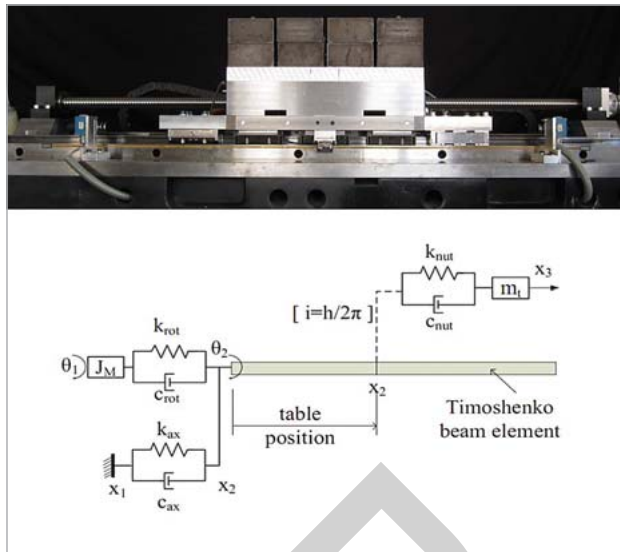


Fig. 1: Experimental set-up of a ball screw axis at the ISW and the corresponding simplified model

culated eigenfrequencies of the simplified model was analyzed afterwards. To obtain the stiffness parameters based on the measured eigenfrequencies, an optimization process was performed using optiSLang. The objective function was defined based on the difference between measured and simulated eigenfrequencies. An extra analysis by means of neural network demonstrated that the correlation between inputs (eigenfrequencies) and output parameters (stiffness) could be determined more robustly via optimization algorithms.

The initial identification of stiffness parameters indicated that, based on the measurement of only two eigenfrequencies, no appropriate stiffness value for the nut could be identified. In order to clarify the correlation, a sensitivity analysis of the model was performed using optiSLang inside ANSYS Workbench. During this sensitivity analysis, different stiffness parameters, as well as the table mass and position, were considered. Furthermore, additional eigenfrequencies were analyzed for calibration of model parameter. The results indicated that neither the first nor the second eigenfrequency was considerably affected by the stiffness of the nut. An additional study was conducted to find a physical vibrational parameter, which is affected by the nut stiffness parameter. The study outcome pointed out that the first eigenmode (machine table movement) is mainly affected by the nut's stiffness. The sensitivity analysis identified three output parameters, which were decisive for the identification of the stiffness parameters of the ball screw drive. Fig. 2 shows the indication represented by optiSLang's Coefficient of Prognosis (CoP) and Metamodel of Optimal Prognosis (MOP) as a result of the sensitivity analysis.

After the modification of the objective function by adding the eigenmodes, as well as the implementation of the correctional factors, the identification of the model param-

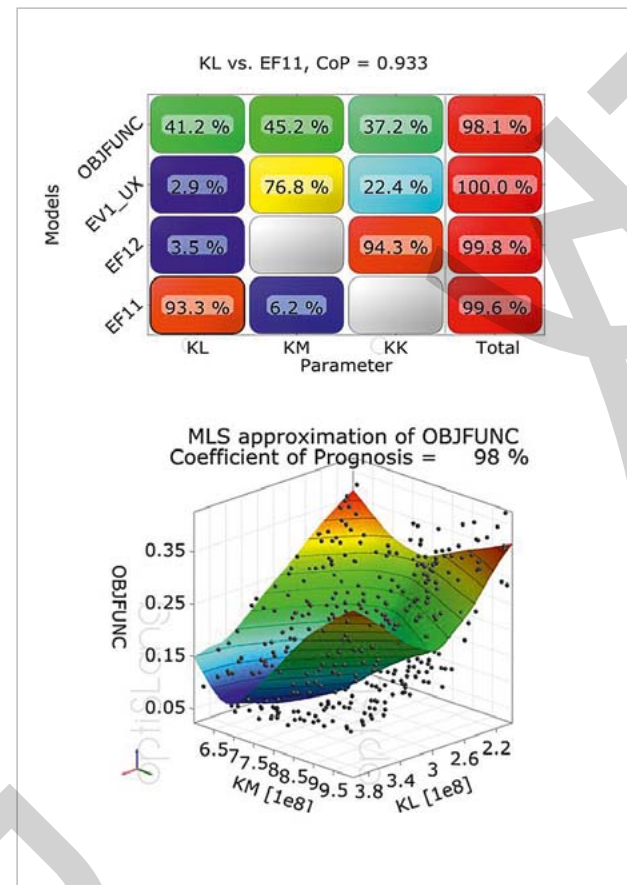


Fig. 2: CoP (left) and MOP (right) based on the sensitivity analysis in optiSLang

eters was conducted. An Evolutionary Algorithm (EA) was applied as a model-based identification algorithm and the stiffness parameters could already be identified after about 200 iterations.

### Accuracy of the algorithm

Fig. 3 illustrates how the proposed SIOCS approach was verified on the basis of the simulation input data. The simplified 2-D model of the ball screw was used to calculate the frequency response of the rotational velocity control. Based on the curve fitting in the Bode plot, the transfer function of the system could then be identified. The eigenfrequencies and eigenvectors were calculated afterwards, using the generated algorithm. By providing the eigenfrequencies and eigenvectors as inputs of the identification algorithm, the stiffness parameters of the ball screw model were determined and the accuracy of the algorithm could be evaluated.

### Conclusion and benefit

As a result of the project, the following conclusions can be drawn: The expected correlation between system parameters and characteristics of the machine could not be determined at the beginning of the project. Only the additional consideration of the system's first eigenmode, as well as the inclusion of a wider range of parameters and system responses identified

by the sensitivity analysis with optiSLang, could explain the phenomena. The correlation matrix showed the interaction between the model parameters and the machine performance. This approach enables an evaluation of the monitored component states by the identification of their real vibration behavior. As a benefit, this allows an optimal adjustment of operating time and maintenance intervals to the current condition of the machine tool.

**Authors //** Mahdi Mottahedi, M.Sc., (ISW, University of Stuttgart)  
Dr.-Ing. Armin Lechler (Chief Engineer, ISW, University of Stuttgart)

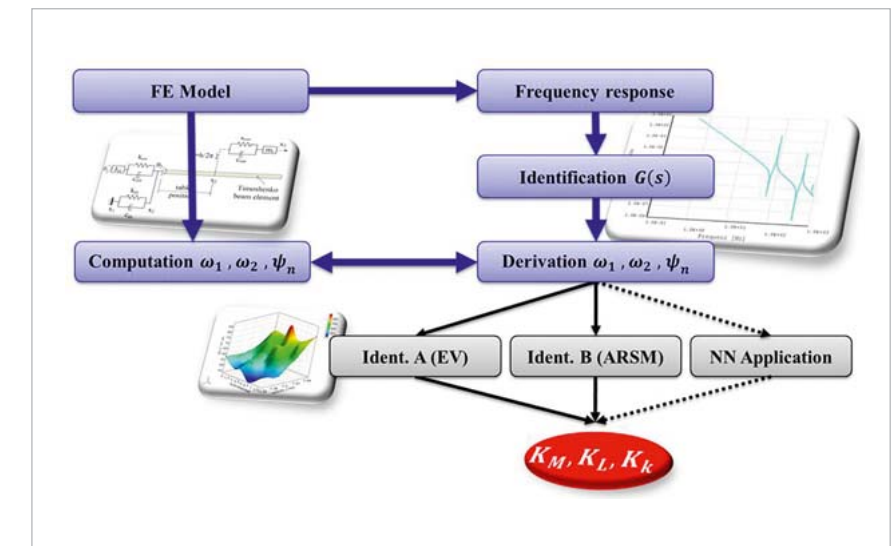


Fig. 3: Workflow of the stiffness parameter identification of a ball screw drive system based on the calculated eigenfrequencies and the second eigenvector

**DYNARDO LIBRARY**

Our internet library is an extensive source for your research on CAE topics and CAE-based Robust Design Optimization (RDO).

[www.dynardo.de/en/library.html](http://www.dynardo.de/en/library.html)



## Contact & Distributors

### Germany & worldwide

Dynardo GmbH  
Steubenstraße 25  
99423 Weimar  
Phone: +49 (0)3643 9008-30  
Fax.: +49 (0)3643 9008-39  
www.dynardo.de  
contact@dynardo.de

Dynardo Austria GmbH  
Office Vienna  
Wagenseilgasse 14  
1120 Vienna  
www.dynardo.at  
contact@dynardo.at

### Germany

CADFEM GmbH  
Marktplatz 2  
85567 Grafing b. München  
www.cadfem.de

science + computing ag  
Hagellocher Weg 73  
72070 Tübingen  
www.science-computing.de

### Austria

CADFEM (Austria) GmbH  
Wagenseilgasse 14  
1120 Wien  
www.cadfem.at

### Switzerland

CADFEM (Suisse) AG  
Wittenwilerstrasse 25  
8355 Aadorf  
www.cadfem.ch

### Czech Republic, Slovakia, Hungary

SVS FEM s.r.o.  
Škrochova 3886/42  
615 00 Brno-Židenice  
www.svsfem.cz

### Sweden, Denmark, Finland, Norway

EDR & Medeso AB  
Lysgränd 1  
SE-721 30 Västerås  
www.medeso.se

### United Kingdom of Great Britain and Northern Ireland

IDAC Ltd  
Airport House Business Centre  
Purley Way  
Croydon, Surrey, CR0 0XZ  
www.idac.co.uk

### Ireland

CADFEM Ireland Ltd  
18 Windsor Place  
Lower Pembroke Street  
Dublin 2  
www.cadfemireland.com

### Turkey

FIGES A.S.  
Teknopark Istanbul  
Teknopark Bulvari 1 / 5A-101-102  
34912 Pendik-Istanbul  
www.figes.com.tr

### North Africa

CADFEM Afrique du Nord s.a.r.l.  
Technopôle de Sousse  
TUN-4002 Sousse  
www.cadfem-an.com

### Russia

CADFEM CIS  
Suzdalskaya 46, Office 203  
111672 Moscow  
www.cadfem-cis.ru

### India

CADFEM Engineering Services India  
6-3-902/A, 2nd Floor, Right Wing  
Rajbhawan Road, Somajiguda  
Hyderabad 500 082  
www.cadfem.in

### USA

CADFEM Americas, Inc.  
27600 Farmington Road, Suite 203 B  
Farmington Hills, MI 48334  
www.cadfem-americas.com

Ozen Engineering Inc.  
1210 E Arques Ave 207  
Sunnyvale, CA 94085  
www.ozeninc.com

### USA/Canada

SimuTech Group Inc.  
1800 Brighton Henrietta Town Line Rd.  
Rochester, NY 14623  
www.simutechgroup.com

### Japan

TECOSIM Japan Limited  
4F Mimura K2 Bldg. 1-10-17  
Kami-kizaki, Urawa-ku, Saitama-shi  
Saitama 330-0071  
www.tecosim.co.jp

### Korea

TaeSung S&E Inc.  
Kolon Digital Tower 2  
10F, Seongsu-dong 2 ga  
Seongdong-gu  
Seoul 333-140  
www.tsne.co.kr

### China

PERA-CADFEM Consulting Inc.  
Bldg CN08, LEGEND-TOWN  
Advanced Business Park,  
No. 1 BalizhuangDongli,  
Chaoyang District,  
Beijing 100025  
www.peraglobal.com

## Publication details

### Publisher

Dynardo GmbH  
Steubenstraße 25  
99423 Weimar  
www.dynardo.de  
contact@dynardo.de

### Executive Editor & Layout

Henning Schwarz  
henning.schwarz@dynardo.de

### Registration

Local court Jena: HRB 111784

### VAT Registration Number

DE 214626029

### Publication

worldwide

### © Images

Fotolia: Cover-J. Vollmer, p. 12-JustContributor, p. 18-julvil,  
p. 22-Cheyenne

### Copyright

© Dynardo GmbH. All rights reserved  
The Dynardo GmbH does not guarantee or warrant accuracy or  
completeness of the material contained in this publication.